Detection of Arcs in Automotive Electrical Systems

by

Matthew David Mishrikey

S.B., Massachusetts Institute of Technology (2002)

Submitted to the Department of Electrical Engineering and Computer Science
in partial fulfillment of the requirements for the degree of

Master of Engineering

at the

MASSACHUSETTS INSTITUTE OF TECHNOLOGY

January 2005

Author .....
Department of Electrical Engineering and Computer Science
January 31, 2005

Certified by .....
Professor Markus Zahn
Thomas and Gerd Perkins Professor of Electrical Engineering
Thesis Supervisor

Certified by .....
Dr. Thomas A. Keim
Assistant Director of the Laboratory for Electromagnetic and Electronic Systems
Thesis Supervisor

Accepted by .....
Arthur C. Smith
Chairman, Department Committee on Graduate Students

Detection of Arcs in Automotive Electrical Systems

by

Matthew David Mishrikey

Submitted to the Department of Electrical Engineering and Computer Science
on January 31, 2005, in partial fulfillment of the
requirements for the degree of
Master of Engineering

Abstract

At the present time, there is no established method for the detection of DC electric arcing. This is a concern for forthcoming advanced automotive electrical systems which consist of higher DC electric power bus voltages, such as the automotive industry proposed 42 volt standard. At these higher voltages, wire faults can lead to stable electric arcs, which may hazardously cause insulation to catch on fire. This thesis presents the results of investigations of phase noise and broadband emissions as indicators of DC electric arcing. We have developed a broadband emissions system based detection system. A proof-of-concept implementation of such a detector indicated favorable results in a laboratory simulated arcing environment, and in a vehicle. Suggestions for robust detection in a noisy environment are presented.

Keywords: 42v, 42 volt, arcing, automotive, broadband, DC, detection, electric, emissions, harness, phase noise, RF

Thesis Supervisor: Professor Markus Zahn
Title: Thomas and Gerd Perkins Professor of Electrical Engineering

Thesis Supervisor: Dr. Thomas A. Keim
Title: Assistant Director of the Laboratory for Electromagnetic and Electronic Systems

Acknowledgments

It has been my pleasure to work with and learn from Professor Zahn and Dr. Keim. Professor Zahn teaches his classes in a way that imparts a love of electromagnetics to his students. Dr. Keim's no-frills approach to problem solving makes others better engineers. They each demonstrate inspiring intelligence and wisdom. Together, their meticulousness and attention afforded the success of this project.

I am also indebted to Professor Dave Perreault and Professor Steven Leeb. I learned from them both inside the classroom, and in LEES. Certain parts of this research would not have been possible without their generous contributions of measurement equipment and supplies. Moreover, when I was confronted with a difficult technical question (often), they shared their valuable time and knowledge.

Finally, a thank-you for Joshua Phinney, for high standards, and comic relief.

To my parents,
Fred and Miriam Mishrikey,
who have made great sacrifices
for our education.

Contents

1 Introduction **1**

1.1 Introduction and Motivation 1
1.2 Previous MIT Research 1
1.3 Thesis Scope 2
1.4 Thesis Organization 3

2 Available Detection Methods **5**

2.1 Technical Literature 5
2.2 Patent Literature 7
2.3 Commercial Arc detection 9
2.4 Review of Possible Solutions 9
2.4.1 Time Domain Reflectometry 9
2.4.2 Phase Noise & Broadband Emissions 10

3 Phase Noise **11**

3.1 Principles of Oscillator Phase Noise 11
3.2 Arcing Phase Noise Measurements 13

4 Broadband Emissions **19**

4.1 Introduction 19
4.2 Measurement Technique 20
4.3 Harness Noise 22
4.3.1 SAE Specifications 22
4.3.2 Calculations Indicating Favorable Signal to Noise Ratio 23
4.4 Voltage Based Detection of Broadband Emissions 24
4.4.1 Voltage Detector 24
4.4.2 Input Filter 24

5 Circuit for Detection of Broadband Emissions **27**

5.1 RF Current Detector Board 27
5.1.1 Buffer 27

5.1.1.1 Estimation of Arc Output Impedance 27
5.1.1.2 Buffer Integrated Circuit 30
5.1.2 Selectivity Filter 31
5.1.2.1 Active Filter Design 31
5.1.3 Power Detection Stage 31
5.1.4 Signal Level Readout 33
5.1.5 Power Supply 33
5.1.6 Board Design and Layout 33

6 Sensing Methods **35**
6.1 Current Clamp Sensors 35
6.1.1 LEM Sensors 35
6.1.2 High Frequency Current Probes 37
6.2 Rogowski Coils and Resonant Sensing 38
6.3 Antenna Sensor 39

7 Detection Circuit Results **41**
7.1 Experiment Test Bench 41
7.2 Distance from Arcing Source Tests 43
7.3 Car Tests 45
7.3.1 Tests with Engine Off 45
7.3.2 Tests with Engine Running 46

8 Conclusions **47**
8.1 Summary of Results 47
8.2 Recommendations for future work 48

A Index of Related Patent Material **49**

B Feedback Analysis of Active Filter **51**

C Partial Datasheet for the LTC5507 **59**

D Decibel Scaling on the Spectrum Analyzer and related equipment **65**

E SAE Table 5 and Calculations **69**

F Schematics and PCB Layout **71**

List of Figures

3.1 Figure adapted from [14], explaining oscillator phase noise. (ARRL Handbook Fig 14.6) . . . 12
3.2 Phase noise representations in time and frequency domain [13] . . . 13
3.3 Crystal oscillator circuit for phase noise measurements . . . 14
3.4 Schematic of measurement of oscillator phase noise . . . 14
3.5 Aluminum Arc Gap . . . 15
3.6 10 MHz oscillator peaking and phase noise shoulders; 13 dB / div . . . 17
3.7 10 MHz oscillator peaking and phase noise shoulders during arcing; 13 dB / div . . . 17

4.1 Schematic of measurement of broadband emissions from an electric arc . . . 20
4.2 Broadband arc gap spectrum: no arcing (10 dB per division) . . . 21
4.3 Broadband arc gap spectrum: with arcing (10 dB per division) . . . 21
4.4 RF bandpass filter circuit model . . . 25
4.5 RF bandpass filter circuit model with parasitics . . . 25
4.6 RF filter model SPICE sweep, $|V_{in}| = 1.0$ [volts] . . . 26
4.7 Filter transfer function measurement on the network analyzer . . . 26

5.1 Main detector circuit schematic . . . 28
5.2 Method for estimating output impedance of an arc . . . 29
5.3 Photograph of Golledge crystal filters . . . 32
5.4 Diode and capacitor peak detector . . . 32

6.1 Current clamp from Solar Electronics . . . 36
6.2 LEM Current Sensors . . . 36
6.3 Open loop LEM sensor diagram . . . 37
6.4 Closed loop LEM sensor diagram . . . 38
6.5 Photograph of constructed Rogowski coils . . . 39

7.1 Schematic of experimental test bench . . . 42
7.2 Probe Master 4251 RF measurement probe . . . 42
7.3 Photograph of detector circuit on test bench . . . 43
7.4 Graph of signal strength vs. distance along conductor . . . 44

B.1 Impedance analyzer sweep of LC tank circuit 52
B.2 Attempted active filter design using LC tank circuit in feedback path 52
B.3 Slew limited oscillation of active filter circuit 54
B.4 Block diagram manipulations for determining L(s) 55
B.5 Bode diagram of the loop transfer function 56
B.6 SPICE probe output of AC Sweep of active filter in Figure B.2; $|V_{in}| = 100\text{mV}$ 57

C.1 LTC5507 Datasheet Page 1 60
C.2 LTC5507 Datasheet Page 2 61
C.3 LTC5507 Datasheet Page 3 62
C.4 LTC5507 Datasheet Page 4 63
C.5 LTC5507 Datasheet Page 5 64

D.1 Spectral Sweep: .105 Vpp input, -15.6 dBm peak 67
D.2 Spectral Sweep: .331 Vpp input, -5.6 dBm peak 67

F.1 Voltage based detector PCB layout 72
F.2 Schematic for original voltage based detector 73
F.3 Final detector PCB layout with ground plane 74
F.4 Final detector PCB layout without ground plane 75
F.5 Schematic for final detector design, repeated from 5.1 76
F.6 Detector photograph, repeated from Figure 7.3 77

List of Tables

E.1 Table 5 from [12]; Narrowband noise limits for automotive loads 69
E.2 Corresponding Voltage [V] level across 50 Ω 69
E.3 Number of noisy loads N necessary to mask arcing emissions 70

Chapter 1

Introduction

1.1 Introduction and Motivation

Automotive groups have been researching a new automotive electrical system standard for almost a decade [18]. A new electrical configuration will be necessary with the introduction of hybrid systems, and because of increased electrical power consumers such as Electronic Valve Technology (EVT) and electric braking.

These changes become necessary as the amount of consumed electrical power approaches the amount available. One simple way to increase the amount of available power is to raise the nominal bus voltage from 14 volts. One of the chosen standards triples the bus voltage to 42 volts.

Reinventing the automotive electrical system forces engineers to confront new problems. One of these problems is DC electric arcing. Newer, higher voltage power systems (such as the proposed 42 volt standard) allow stable, self-maintaining electrical arcing to occur, whereas conventional 14 volt systems do not. Arcing can occur when electrical circuits are short circuited, or when wire or wire insulation is damaged.

In the initial MIT studies to characterize arcing, Wu showed 36 volt arcs to be 1 to 2 orders of magnitude more energetic than their 12 volt counterparts [2]. As such, the risk of fire (started by burning insulation) or gas-fume explosion is much greater. To implement a new auto standard, this critical safety hazard must be overcome.

If, as in the case of a vehicle collision, wires are unpredictably cut and circuits are shorted, we must have a strategy to detect arcing and prevent its potentially continuous existence (stable arcing) or repeated restarts (intermittent arcing). At the present time, we are aware of no such implemented solution. The criteria on which one can judge a detection solution include speed, ability to localize where an arc is happening, and accuracy of detection.

1.2 Previous MIT Research

Two previous MIT graduate students have contributed to arcing detection research.

Alan Wu studied the behavior of fuses under the circumstances of intermittent arcing [22]. He determined parameters such as RMS current, peak current, and arc duration required

to blow various fuses. He then demonstrated that intermittent stable arcing which did not exceed those parameters did not blow respective fuses.

Further, Wu compared 36 volt and 12 volt arcing. He found that 36 volt arcs contained up to two orders of magnitude more energy than their 12 volt counterparts, and resulted in commensurate physical damage. Wu also states that the 36 volt arcs he produced were more likely to form welds, allowing fuse-blowing currents and mechanically preventing continued intermittent repetition.

Joseph Luis attempted electronic detection of arcs. Using an improved drawn arc apparatus, he created stable arcs and measured their current profiles. He analyzed these currents in the frequency and time domains, and determined that those methods of analysis were not sufficient to detect arcing. He found that arcs were too random in their behavior, and that their frequency spectra were not significantly distinguishable from those of normal automotive loads ([8], p. 83).

Specifically, Luis claimed that "the frequency spectrum of arcing current shows *broadband characteristics* with no significant or distinguishing characteristics that can be used for simple detection of all arcs." Broadband characteristics of arcs are reconsidered in this thesis.

He found that certain loads, such as ones which utilize pulse width modulation (PWM), produce recognizable patterns which allow these loads to be eliminated as false positives. Along these lines, he suggests the possibility of signing all loads with unique markers. Any transients occurring without a marker would then be related to an arc event. This strategy, however, still requires an exact characterization of all transients, many of which have a nondeterministic and therefore non-characterizable behavior.

1.3 Thesis Scope

This thesis includes the investigation of oscillator phase noise as a means of detecting arcing. Broadband emissions were also considered. A broadband emissions based arc detector was designed and tested. This thesis also discusses detection in a noisy background environment, as well as sensors useful for detection and emissions measurements.

This thesis does not cover the topic of localization of arc faults, though some mention is given to this in the Conclusions chapter. Also, no material is devoted to circuit breakers or redundancy strategies necessary for the mitigation of arc faults.

1.4 Thesis Organization

The next chapter covers available detection methods provided in patents, journals and conference proceedings, as well as prior art technology. It also contains a brief overview of approaches we considered at the outset of the research.

Phase noise and phase noise measurements during DC electric arcing are discussed in Chapter 3.

A discussion of measurements of broadband noise is given in Chapter 4. Additionally, there is a discussion regarding the detection of broadband emission noise in the presence of other background noises.

Chapter 5 offers a thorough description of our proof-of-concept broadband emissions based detector circuit. It also notes which simplifications were made and suggests adjustments necessary for an actual detector design.

Sensing techniques necessary for the detection of broadband emissions are covered in Chapter 6.

Results of tests performed using the detector are in Chapter 7. This includes detection tests on the live harness of a Toyota Corolla.

An overview of what was accomplished is given in the last chapter. Also, ideas for future research in this area are presented.

The appendices include relevant technical notes and circuit schematics.

Chapter 2

Available Detection Methods

This chapter is intended to supplement Chapter 3 on detection methods in [8], which gives a good overview of electronic detection in AC and DC systems using acoustic, electromagnetic, and optical detection methods.

Additionally, this chapter offers a brief overview of the possible approaches we considered as solutions to the arcing problem. In the final section of the chapter we discuss an approach we considered but did not pursue. We also introduce two options explored during the course of this research, which are further discussed in their own chapters.

2.1 Technical Literature

This section covers published technical papers on the topic of arc fault detection.

***Mitigation and analysis of arc faults in automotive DC networks*; Schoepf, Naidu, et al.**

Schoepf, Naidu, et al. give a good overview of the two types of arc faults (serial and parallel), and cite several sources which performed fault simulations, including various mechanical failure and water intrusion tests [16]. The publication also gives mention to some failure mitigation problems such as redundancy in X-by-wire systems. It also reiterates Wu's findings that fuses and circuit interrupters may not clear faults (and never do, in the case of series faults).

Presented are two detection concepts. "Zone arc detectors," which simply observe differential current and voltage measurements, and "current signature detectors," which observe the nature of arcing current signals.

Accurately stated are the several flaws of differential measurement based arc detection, the most fundamental of which being that these methods only guard a designated protection zone which is necessarily less than the entirety of the circuit. Harness conductor terminations, for example, are generally not easy to enclose within such a protection zone. This is inadequate, as a major class of arc faults stems from undesired connector separation.

Schoepf goes on to outline current-signature topologies, using a single toroidal transformer as a sensor. Unfortunately, no explanation is given as to how circuitry distinguishes arcing transients from allowed ones. Only the following acknowledgment is presented:

> "[Sensed] signal is fed to the processing control circuitry where it is compared with a specific threshold to generate a trip signal for the relay ... signal processing is more complex [in contrast to differential measurement methods] as current ripple (noise) must be filtered in normal operation mode, e.g. motor commutation. The toroidal coil and the control circuit incorporate means to distinguish between normal current ripple and current waveform changes due to real arc faults."

The bulk of this thesis aims to fill in this void by giving a detailed description of how to discern arcing and normal load transients.

The rest of [16] covers experimental tests using an implementation of each detector variant with several types of loads under various fault conditions. Comparisons are made between connector damage with and without arc fault protection. It is however not clear these comparisons take into account false-positive activations of the detectors.

***Design and Analysis of Aerospace DC Arcing Faults using Fast Fourier Transformation and Artificial Neural Network*; Momoh and Button**

One interesting idea was published after we had already made progress with our own detection strategy.

Momoh and Button propose a DC arc fault detection system for aerospace electrical networks [9]. For small spacecraft, these are generally 28 volts DC. Test data was obtained from NASA Glenn Research Center on arcs generated on 50 to 150 volt DC busses.

The system proposed uses "fast fourier transform (FFT) based spectrum estimation to analyze the recorded signals of DC arcing faults," in conjunction with an artificial neural network (ANN) trained to discern arcing patterns from normal ones.

The output of the ANN is a single neuron, and the input layer consists of 10 neurons whose inputs are "the energy of frequency components obtained [from] the FFT DSP module." It is not clear to the reader what operation is performed on the arcing signal or the FFT of the arcing signal to process it for input to this ANN.

The detection system was trained and tested on roughly 240 and 60 recorded arcing signals respectively. These tests were limited to computer simulations; no detection system was used to detect live arcs. The authors claim that this method is accurate and fast, however no statistical data or calculation speed is given for these trials. A subset of trial results shows a 30 percent failure rate (with every failure being a missed detection).

***Investigations into electromagnetic emissions from power system arcs*; Vaughan, Moore, et al.**

Vaughan, Moore, et al. discuss broadband emissions caused by arcing sources and define "sferics" as low frequency atmospheric waves which can travel long distances [20, 21]. Using sferics, the authors attempt to detect arc faults in electric power distribution stations. The concept for this was inspired by similar lightning detection systems. The results of this

research may be useful for developing immunity specifications for local broadband emissions detectors, such as the one described in this thesis.

The research conducted focuses on very low frequencies (VLF), using 9 meter long antennas, but mention is also given to a 50 MHz data acquisition system using a 3 meter long antenna (half-wavelength).

Also addressed is the topic of localization by triangulation. This is similar to acoustic triangulation as discussed in [8]. As electromagnetic waves travel at the speed of light, and not the speed of sound, monitoring stations are spaced farther apart. Tests performed on using these monitoring stations showed that switching induced sferic radiation can be observed up to one kilometer away from arcs.

2.2 Patent Literature

There is an abundance of patent material in the area of arc detection, however only a small portion of these are devoted to detection of arcs in DC electrical systems. For convenience, a listing of arc detection related patent numbers and titles is included in Appendix A. In this section we will consider three particularly interesting patents.

***Detection of arcing faults using bifurcated wiring system*, US Patent No. 6,782,329**

US Patent No. 6,782,329 [17] presents a variant on conventional differential current measurement systems, mentioned in Section 2.1. The standard differential system measures the currents through and voltages at either end of a protected conductor. Parallel faults are detected upon a non-zero differential current measurement, and series faults, which represent voltage drops, are detected upon a non-zero voltage difference.

The bifurcated wiring system is similar. A protected conductor is replaced by two identical conductors, each with half the cross-sectional area of the conductor being replaced. Current sensors then check each branch of the bifurcated conductor for a difference in current, as opposed to checking the two ends of a single conductor.

While this variant may offer certain geometric advantages (for example: current sensors can be placed in the middle of the conductor, close to one another), it has the same disadvantage as with other differential systems; arcs in the circuit outside the protected (or in this case, bifurcated) region cannot be detected.

This topology also presents a unique disadvantage. Series or parallel faults in the bifurcated zone which result when both branches are identically severed may not be detectable.

***DC arc detection and prevention circuit and method*, US Patent No. 6,683,766**

US Patent No. 6,683,766 [1] gives specific mention of the 42 volt automotive application in

its background section. This invention claims to detect precursors to imminent arcs, such as step transients in current waveforms. It also presents a method for preventing an arc from forming. When an arc precursor is sensed, a command signal is sent to a switching circuit instructing it to momentarily shut off. The command specifies the duration of the shutoff necessary for preventing an arc.

The momentary shutoff is described as being long enough to allow an sufficiently large air gap to form between connectors, and short enough that loads are not unnecessarily cutoff from power. This implies that one aim of the invention is to allow momentary disconnects. Also mentioned in the description is an optional microprocessor which decides if too many disconnects have occurred and the circuit should be more permanently switched off.

A major question left unanswered is how this invention discerns load transients from arcing ones. All that is clear from the description and claims is that an arc precursor condition consists of either a change in conductor current or a change in voltage at the location of the imminent arc.

***Electric Arc and Radio Frequency Spectrum Detection*, US Patent No. 5,477,150**

US Patent No. 5,477,150 [4] states that

> "A principal object of the invention is to detect sparks or arcs in electric circuits or otherwise to detect a spectrum of a broad band of distinct instantaneous radio frequencies in radio frequency noise."

This invention works by detecting broadband RF emissions. The preferred embodiment functions by using a ferrite core RF transformer for pickup, but specifically states that this could be replaced by an antenna, near field capacity coupler, or another type of RF energy pickup.

The invention presents a strategy for rejecting extraneous narrowband signals from non-arcing sources by using a balanced mixer configuration which tends to cancel out narrow-band inputs, but not broadband ones. In this thesis research, another method is used for filtering and detection. Frequency sweeps or sampling multiple distinct narrow bands of filter signals are used as a solution for rejecting spurious narrowband inputs.

This thesis presents a very specific detector implementation and provides a good starting point for development of detection applications. Additionally, this thesis offers an in depth discussion of filtering strategies, practical methods of RF sensing, and noise specifications. Particular attention is given to the automotive application of these methods. Also, new possibilities such as phase noise detection of arcs are presented.

2.3 Commercial Arc detection

It should be mentioned that arc detectors exist in commercial form, for AC power frequency applications. In fact, many states now require the use of arc fault circuit interrupters (AFCI) January 1st, 2002, as recommended by the National Electric Code (NEC) [10]. The relevant portion of the NEC gives the following definition and prescription:

> 210.12 Arc-Fault Circuit-Interrupter Protection.
>
> (A) Definition. An arc-fault circuit interrupter is a device intended to provide protection from the effects of arc faults by recognizing characteristics unique to arcing and by functioning to de-energize the circuit when an arc fault is detected.
>
> (B) Dwelling Unit Bedrooms. All branch circuits that supply 125-volt, single-phase, 15- and 20-ampere outlets installed in dwelling unit bedrooms shall be protected by an arc-fault circuit interrupter listed to provide protection of the entire branch circuit.

Luis offers a good overview of AC detection methods [8], and explains why these methods do not carry over to DC arc detection. In particular, many AC methods rely on changes in zero crossing behavior, or arc induced asymmetry in AC waveforms. Neither of these indicators are manifested in DC arcing.

2.4 Review of Possible Solutions

2.4.1 Time Domain Reflectometry

One strategy avoids the complexities and randomness of arcing behavior by looking for faults instead of arcs. We can treat a wiring harness as a network of transmission lines. For a simple transmission line, it is easy to detect how the transmission line is loaded by applying a pulse to the transmission line and measuring reflections of that pulse. This method is know as time domain reflectometry (TDR).

TDR systems have been used for finding faults in power distribution lines, television cable, intercontinental deep-sea cabling, and the like. Commercial equipment is available for these applications, but this method has not been applied to automotive harnesses. US Patent 5,268,644, titled "Fault Detection and Isolation in Harness by TDR," presents this idea [5], but no specific implementation or research is available.

In conventional TDR systems, a transmission line is first removed from its power source, then connected to test equipment. Because many faults remain hidden when no arcing is occurring, TDR equipment is often used in conjunction with devices called "thumpers." These send a strong pulse of power intended to cause faults to arc over, immediately before TDR pulses are applied. These methods are suitable for offline testing of harnesses. For our

purpose, it is necessary to develop a TDR system which can be used in a live harness, or another system which can recognize arcing in real time. TDR could then be used afterwards for localization.

Two major difficulties need to be addressed before TDR can be successfully applied to automotive harnesses. The first is the sheer complexity of cable harnesses. While these can be broken down and idealized into networked transmission lines, such a model may not be easy to apply when measurements are obfuscated by multiple reflections from hundreds of impedance changes. Another problem is the presence of noise, including switching noise, PWM noise, and electromagnetic interference. All of these may adversely affect reflection tests.

We presented our ideas on TDR detection at a subcommittee meeting of the MIT Consortium in Tokyo, in October 2003. Two noteworthy ideas were presented to us at this meeting; detection of phase noise and detection of broadband emissions. While we do not discount the possibility of a TDR system, we wanted to optimize our chances of creating a successful detector. In light of difficulties associated with TDR detection, and the potential of the two new ideas presented, we decided to pursue those possibilities instead.

2.4.2 Phase Noise & Broadband Emissions

The first recommendation, that arcs may elevate oscillator phase noise levels, is presented in Chapter 3.

The second recommendation, that arcs exhibit broadband emissions which may be used for detection is presented in Chapter 4.

We were unable to produce the described phase noise effects, however this material is presented as a reference for further exploration.

The broadband emissions approach, on the other hand, appeared to be feasible after taking initial measurements. A detector design is presented in subsequent chapters.

Chapter 3

Phase Noise

A meeting of the MIT Consortium's research unit "7b.1" subcommittee, responsible for investigating arc detection, was conducted in Tokyo in October 2003. At that meeting it was suggested that elevated levels of phase noise are associated with arcing[1]. Specifically, when a conductor is injected with a sinusoidal current and an arc occurs, the physical phenomenon of arcing may have a dispersive or frequency-spreading effect on this current. This dispersion would manifest itself as visible "phase noise shoulders," discussed further in this chapter.

We found no literature references to support this suggestion. Encouraged by this idea however, we decided to pursue the possibility of phase noise as a means of detection by taking phase noise measurements. Our measurements neither confirmed nor denied an increase in phase noise. They showed that phase noise effects, if any, were hard to detect in the presence of broadband emissions.

Because broadband emissions seemed more promising, we ultimately pursued that direction instead. Our experiments in phase noise were still useful, and are documented in this chapter for those intending to undertake a more vigorous characterization of phase noise during arcing.

3.1 Principles of Oscillator Phase Noise

Phase noise in an oscillator is caused by perturbations of an oscillator's output [14]. When we depict oscillator voltage amplitude and angle in a phasor plot, phase noise can be drawn as a random variation in the phasor angle. Figure 3.1, adapted from [14], demonstrates this. Figure 3.1 (A) depicts the phasor representation of the oscillator, while Figure 3.1 (B) shows how noise is a cloudy uncertainty in the position of the tip of the voltage phasor. Figure 3.1 (C & D) differentiate phase noise from amplitude noise.

Phase noise can be alternatively represented in time and frequency domain plots. In the time domain, phase noise manifests itself as a horizontal "jitter". A cartoon representation of this is shown in Figure 3.2. In the frequency domain, observation of a low phase noise oscillator with a spectrum analyzer shows a sharp spike at the center frequency f_0. If however, the oscillator is not perfect and produces phase noise on its output, we will see phase noise "shoulders" surrounding the center frequency spike.

[1] We are particularly grateful to David Pommerenke of UM Rolla for these ideas

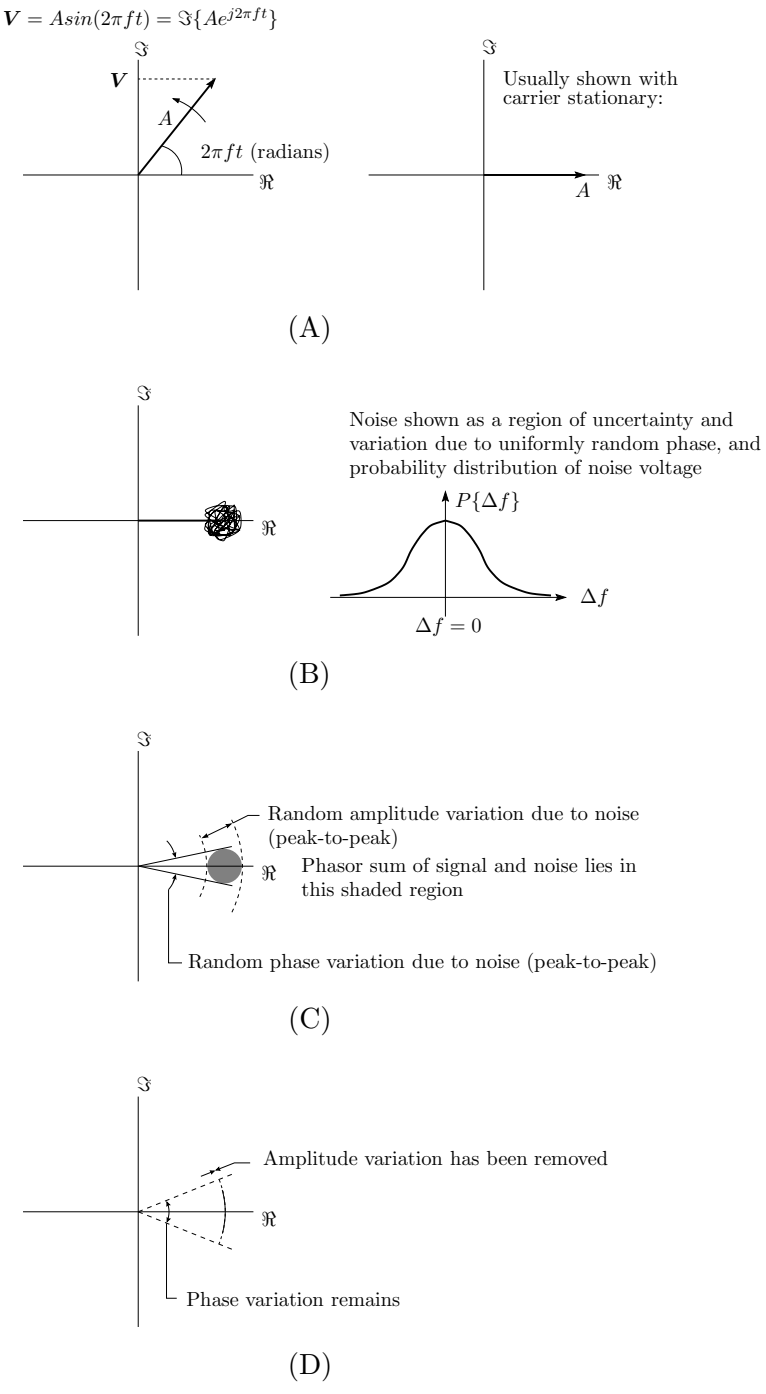

Figure 3.1: Figure adapted from [14], explaining oscillator phase noise. (ARRL Handbook Fig 14.6)

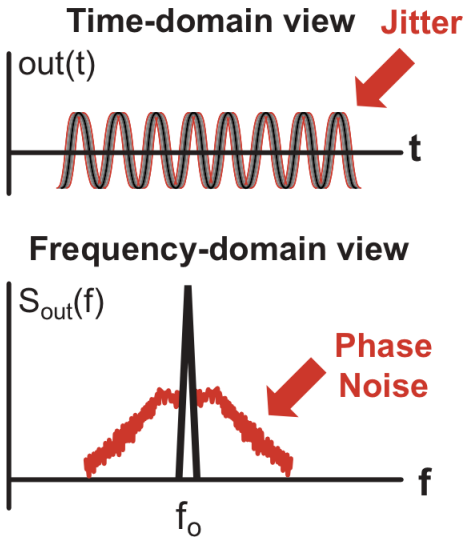

Figure 3.2: Phase noise representations in time and frequency domain [13]

In [6], Lee and Hajimiri use a simple model to describe second order roll-off behavior in phase noise shoulders. The model consists of a simple lossy oscillator and uses the thermal noise of the lossy element as the noise source.

3.2 Arcing Phase Noise Measurements

To take phase noise measurements during arcing, we made arcs in an oscillator driven circuit.

It is important to make sure that the phase noise of the oscillator is smaller than the phase noise which may be produced by the arc. Initially we began our experiments with a high quality signal generator with good phase noise specifications (an SRS DS345 function generator, specification: $<$ -50 dBc in 30kHz, measured: $<$ -90 dBc in 30 kHz). Later, for comparison purposes, we used a crystal oscillator circuit as shown in Figure 3.3. The crystal oscillator produces many extraneous harmonics, however the fundamental frequency was as good as the function generator as a low phase noise source. For these tests we used a 10 MHz signal frequency, which was within the capabilities of the function generator. This was an arbitrary selection; phase noise may be more apparent at other center frequencies. This is one possibility to explore in future arcing phase noise research.

We connected the oscillator signal to an arc gap as shown in the schematic of Figure 3.4. The arc gap is made of two 25 millimeter squares of aluminum, separated by a .5 millimeter air gap. A photograph of the arc gap is shown in Figure 3.5. In parallel with the arc

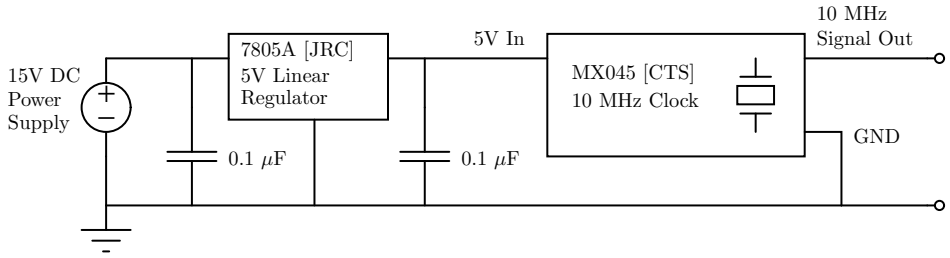

Figure 3.3: Crystal oscillator circuit for phase noise measurements

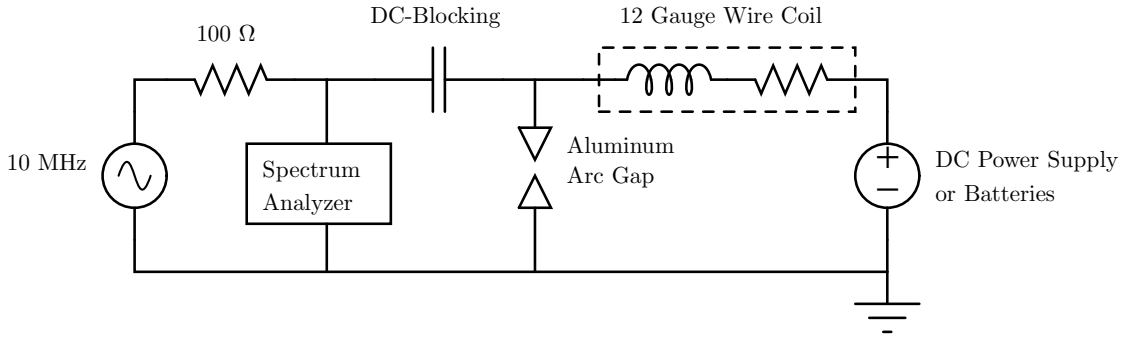

Figure 3.4: Schematic of measurement of oscillator phase noise

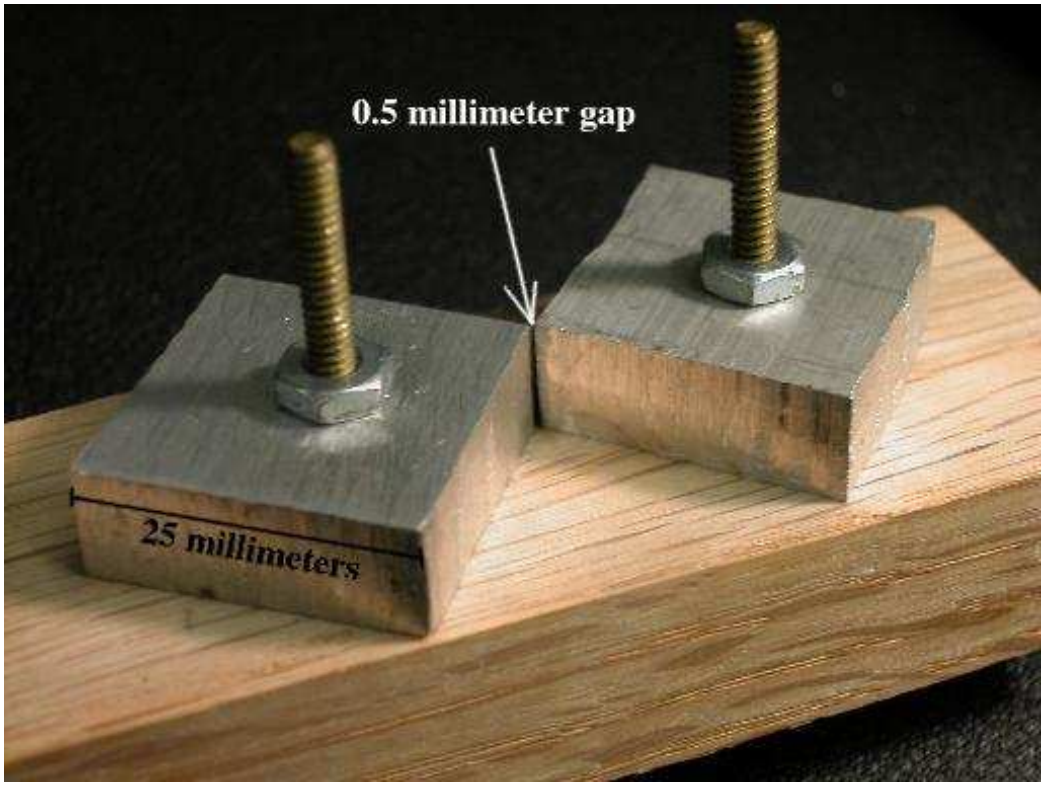

Figure 3.5: Aluminum Arc Gap

gap is a high power DC power supply (Hewlett Packard Model HP6477C), set to 40 volts, in series with a coil of current limiting wire. The coil has a measured inductance of 7 microhenry, and a resistance of 0.3 ohm. The 100 ohm resistor in Figure 3.4 allows for a voltage difference between the oscillation source and the arcing side of the circuit. A series of capacitors provides DC protection for the measuring instrument, an Agilent 4395A spectrum analyzer. The 4395A will display its input noise power as a function of frequency. Its operational frequency range is from 100 kHz minimum to 500 MHz maximum.

To initiate an arc, we brush the arc gap using the frayed end of a piece of stranded wire. A stable arc lasts for several seconds, at which point the arc gap has eroded and oxidized to a point where the arc can no longer continue. Alternatively, we can extinguish the arc by manual interruption (turning off the DC power source), once we have taken a spectral snap shot of the AC arc voltage.

Figure 3.6 shows the 10 MHz oscillator peak without arcing. There is a small amount of "shouldering" where the base of the 10 MHz peak meets the noise floor. Figure 3.7 is a snapshot measurement of the same operating setup during arcing. The biggest observable difference is an increase in the noise floor level, by approximately 1 vertical division.

The increase in phase noise is not clearly visible. There may be added power in the shoulder regions of the arcing snapshot, but it is hard to differentiate this from the raised noise floor. Also, because of noise variations from sweep to sweep, it is necessary to compare averaged sweeps instead of single spectral snapshots. Even with averaging, the difference in phase noise may be too small to be reliable.

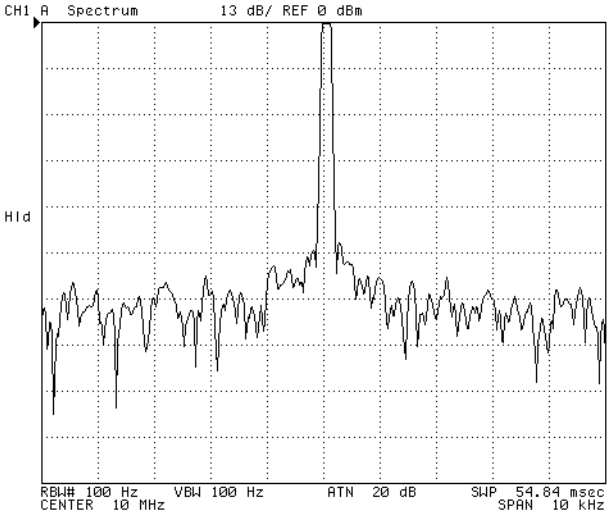

Figure 3.6: 10 MHz oscillator peaking and phase noise shoulders; 13 dB / div

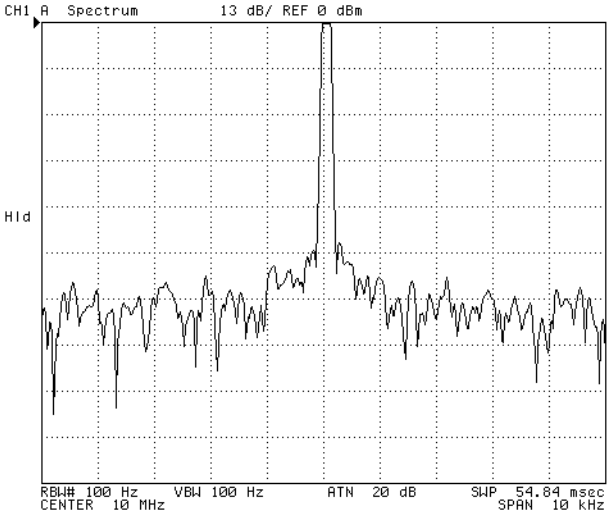

Figure 3.7: 10 MHz oscillator peaking and phase noise shoulders during arcing; 13 dB / div

One property of arcing, however, which we may be able to exploit is the noticeable difference in noise floor level. When we repeated these tests using a wider sweep range, this difference became more pronounced. This corresponded with larger integration intervals into which the spectrum analyzer accumulated noise. This topic is continued further in Chapter 4.

Chapter 4

Broadband Emissions

4.1 Introduction

This chapter discusses the measurement of noise produced by DC electric arcing.

Numerous sources suggest that arcs are good sources of broadband noise. Guglielmo Marconi used spark-gap transmitters for wireless communication in the early 1900's [14]. These devices used arcs to excite antennas which would transmit broadband signals. Ragnar Holm describes radio noise produced by arcs, gives a plot of an arc noise spectrum (see [2], Figure 47.08), and gives suggestions for reducing arc noise in commutator systems ([2], p. 273). Research on RF arc detection for the DIII-D Tokamak fusion project states that arcs generate broadband noise ([15], p. 522).

Taking advantage of noise as a phenomenon to detect is an attractive solution. Unlike alternative methods relying on a visible or audible link to the arc event ([8], pp. 3, 17), electrical detection does not mandate line of sight or sound.

Another feature of the broadband noise method is that it can detect both series and parallel arc faults. Methods relying on differential current measurements cannot detect series arc faults because currents entering and exiting a series arc are identical. By inspecting spectral behavior of these currents, and not the amount of current flowing, we bypass this limitation.

In his work on automotive arc detection, Luis found that "arcing current does not exhibit a sufficiently large and distinct arcing signature" ([8], p. 83). One reason to look beyond this conclusion is that spectral analyses performed in [8] were limited to a small frequency range and thus were not highly sensitive to broadband emissions. Most fast fourier transforms (FFT's) and periodograms were calculated only up to 3 kHz.

Another difficulty with the previous research was that calculations were performed exclusively using drawn arc current profiles. It was necessary to discriminate between step transients in current and arcing signals. It was also necessary to consider the continuously changing length of the drawn arc as a variable affecting these measurements. For broadband emission measurements in this research, as with phase noise measurements discussed in Chapter 3, we avoid this problem by using a stationary arcing apparatus, and by taking measurements only during the stable formation of an arc.

This chapter will discuss the measurement of broadband emissions, the feasibility of measuring broadband noise in an already noisy environment, and a proof of concept voltage

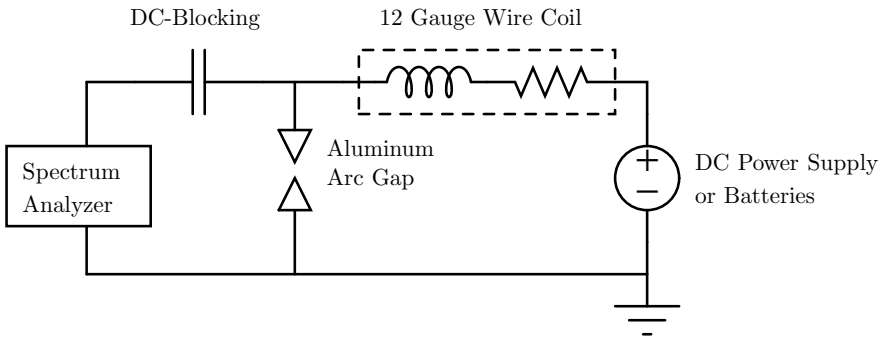

Figure 4.1: Schematic of measurement of broadband emissions from an electric arc based detector.

4.2 Measurement Technique

Measuring broadband emissions follows a procedure similar to the one taken for measuring phase noise. To observe broadband emissions, however, we inspect a much wider frequency range than that observed for phase noise measurements.

Using an experimental setup as depicted in Figure 4.1, it is easy to see the effect of broadband noise during arcing. Figure 4.1 differs from Figure 3.4 in that the oscillator has been removed. Figure 4.2 shows the broad spectrum (500 kHz - 100 MHz) of the AC voltage across the arc gap, without arcing.[1] After initiating an arc and repeating the measurement, we notice a significant change in the arcing spectrum in Figure 4.3.

[1]Due to an Agilent documented measurement phenomenon in the spectrum analyzer, there is a step deviation near 10 MHz. This will not affect a qualitative analysis of our measurements.

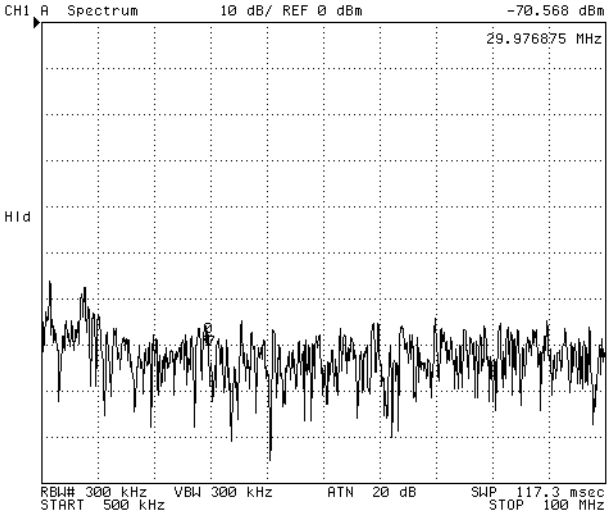

Figure 4.2: Broadband arc gap spectrum: no arcing (10 dB per division)

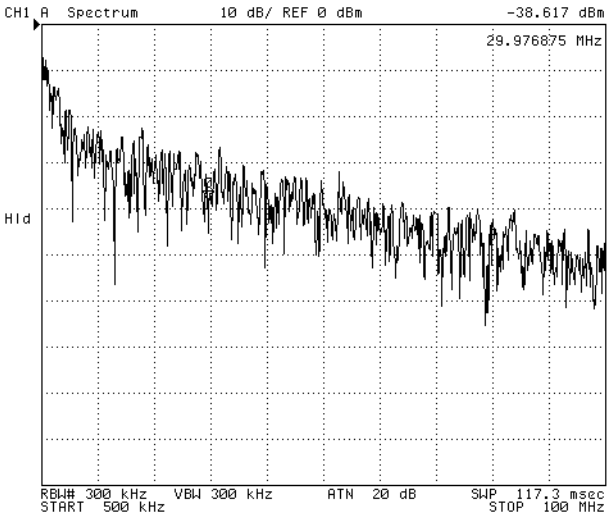

Figure 4.3: Broadband arc gap spectrum: with arcing (10 dB per division)

As seen by the marker measurements near 30 MHz, spectral power in the 300 kHz region of measurement near 30 MHz jumps from near -70 dBm to approximately -38 dBm with an . This difference is quite large and exceeds variations in the noise floor. More importantly, this measurement is repeatable every time a stable arc is present.

For the purposes of demonstrating the emissions detection technique, we started by working with high voltages and currents to produce favorable measurement conditions. An important question to consider is whether it would be possible to notice these changes in broadband emissions if the arcs were of lower energy.

One way to check this is by adding a series resistance to limit the arcing current. We were able to obtain similar broadband emissions with as much as 3 ohms of limiting resistance. We brought this down to 2 ohms to allow us to more readily ignite stable arcs. Arc current limited by a 2 ohm series resistance are small "fizzles" as compared to arcing without added series resistance. That is, they are much smaller, and quieter. Additionally, they perform less damage to the arcing electrodes; less material moves from one electrode to the other. For experimentation, this allows us to use the arc gap electrodes longer, before they become too deformed and corroded to be useful.

We cannot measure voltage directly across an arc in an automotive system, since we cannot predict where an arc will happen on the harness. Therefore, we would like to rely on arcing current to find broadband noise. Voltage measurements will still be useful for studying emissions as a means of detection.

4.3 Harness Noise

If we are to use the existence of high frequency spectral power as a detection criterion for automotive arcs, we must be certain that noise in frequency ranges we are interested in is not produced by standard automotive loads. For example, arcing from alternator commutator brushes and switching from PWM loads may introduce their own high frequency noise which would negatively affect our detection process.

4.3.1 SAE Specifications

One way to determine if automotive loads are an issue is by measuring spectral power at detection frequencies, with no arcing present. If power from arcing broadband emissions greatly exceeds harness noise power at those same frequencies during normal, non-arcing operation, then the detection method is viable.

It is possible to make such a comparison without taking any measurements. The Society of Automotive Engineers has a noise requirement standard, SAE J1113/41 [12] which specifies

EMI noise requirements for 14 volt loads.[2]

According to Table 5 of the SAE standard, conducted emissions in the frequency range of 30-54 MHz may not exceed 52 microvolts into a 50 ohm load. This standard applies to class 1 loads, the most lax of the 5 J1113/41 specified load classes.

4.3.2 Calculations Indicating Favorable Signal to Noise Ratio

In this section we will compare the SAE specifications to spectral measurements on broadband noise as an approximation of expected signal to noise ratio.

From Figure 4.3, we see that spectral power near 30 MHz into the 50 ohm input terminal of the spectrum analyzer is approximately -38.6 dBm. Equations 4.1 and 4.2 define absolute units of power and voltage in terms of their relative counterparts.

$$P[mW] = 10^{\frac{P[dBm]}{10}} \tag{4.1}$$

$$V[\mu V] = 10^{\frac{V[dB\mu V]}{20}} \tag{4.2}$$

The time average input power, P_{in}, dissipated in the input of the analyzer is related to RMS voltage V_{in} across the analyzer input resistance of 50 ohms by the following equation.

$$V_{in} = \sqrt{50 \cdot P_{in}} \tag{4.3}$$

Combining Equations 4.1 and 4.3, we find that voltage across the 50 ohm spectrum analyzer input is

$$V_{in} = \sqrt{50 \cdot \frac{10^{-38.6/10}}{1000}} [volts] \tag{4.4}$$

$$V_{in} = 2.63[mV] \tag{4.5}$$

If we assume noise from loads in the car is uncorrelated, we can calculate the number of loads N necessary to produce arcing levels of noise by Equation 4.6

$$N = \left(\frac{Arc\ Noise\ Voltage\ Level}{Load\ Noise\ Voltage\ Level} \right)^2 \tag{4.6}$$

[2]We are comparing noise from 14 volt loads and the same from 42 volt arcing. As noise standards may be more lax in a future 42 volt specification, we are merely using the 14 volt standard to make a first order approximation of the viability of this method.

If we are conservative in our comparison and assume that all loads are class 1 loads having emissions at the standard's limit of 52 dBμV (398.1 μV) at 30 MHz, then it will take $N = (2.63{\cdot}10^{-3} \div 398.1{\cdot}10^{-6})^2 \simeq 44$ such loads to produce the same emissions power as our arc tests did at 30 MHz. Further, if we assume detection is possible at a signal to noise ratio of 2, then the number of loads it will take to trigger a false positive on a detector is $44 \div 2 = 22$.

By this estimate, we determined that using broadband emissions for detection is a worthwhile approach. It will however be necessary to characterize conducted emissions from standard automotive loads to check the accuracy of these sensitivity estimates.

4.4 Voltage Based Detection of Broadband Emissions

Based on our findings on broadband emissions, we successfully designed and built a proof of concept voltage based broadband emissions detector. This was the first stage in an evolving detector design. The final design is thoroughly discussed in Chapter 5. For completeness, schematics for the voltage based detector are included in Appendix F, and a brief discussion of relevant design details follow.

4.4.1 Voltage Detector

To access the arcing voltage, alligator clips were connected directly to the electrode bolts of the arc gap shown in Figure 3.5. Then, using a series 0.22 microfarad DC blocking film capacitor, the AC arcing voltage was connected to the spectrum analyzer using a short BNC cable terminated with a BNC to N-type connector.

Unlike standard RF measurements using the spectrum analyzer, no effort was made to ensure that the line impedance of the connection was matched with the input impedance of the analyzer, or the output impedance of the arcing source. This is because the arcing source does not have a constant impedance; it is chaotic and cannot easily be matched.

The significance of this is that the signal being measured on the spectrum analyzer may include reflections representing transmission artifacts of the original signal. This does not effect our use of broadband emissions as a detection variable, as we were able to detect differences between arcing and non-arcing using this configuration. It does however affect our interpretation of these measurements as an actual representation of the arcing voltage.

4.4.2 Input Filter

The first stage of detection is the input filter. For the voltage detector, we designed a passive filter and will discuss it here. Detection topology and circuit design is discussed in

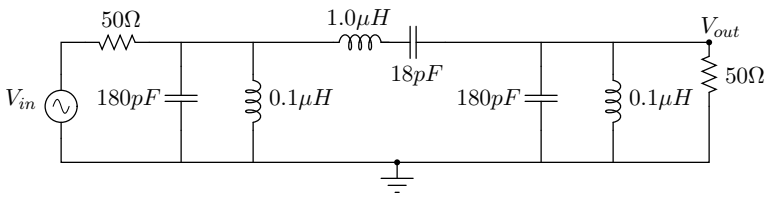

Figure 4.4: RF bandpass filter circuit model

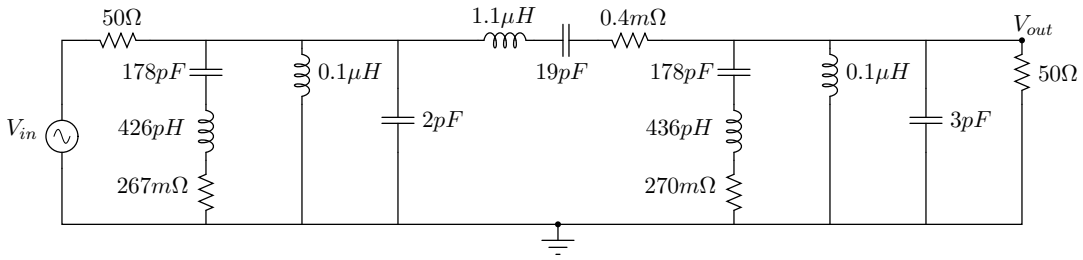

Figure 4.5: RF bandpass filter circuit model with parasitics

a complete manner in Chapter 5.

We used a symmetrical "Pi Filter", frequently discussed in filter design textbooks (See [19]). Our design constraints were minimal; while we required -3 dB points to be near 30 and 50 MHz, we had no strict requirements on passband or stopband shape. We found a suitable filter design which met our requirements but with a passband between 21 and 30 MHz [11]. We then altered component values to shift and scale the passband to meet our specifications. A schematic of this model is shown in Figure 4.4.

We made a PSpice model of the resulting circuit. After running this model through a simulation, we adjusted the model by adding parasitics which would make it more closely resemble the network analyzer output. This is not a necessary procedure, but rather a good exercise which gives us faith in our measurement procedure, and our circuit model.

Figure 4.5 shows this model circuit with the added parasitics. As can be seen from the PSpice simulation in Figure 4.6, the circuit models a bandpass filter with the desired frequency range.

Figure 4.7 shows the network analyzer sweep of the assembled filter. The filter shape of the bandpass region and the PSpice simulation match closely. Five higher order "peaks" are seen after the bandpass region, starting at 100 MHz. These peaks represent transmission line effects of our measurement apparatus, and have no bearing on the filter's use in emissions detection.

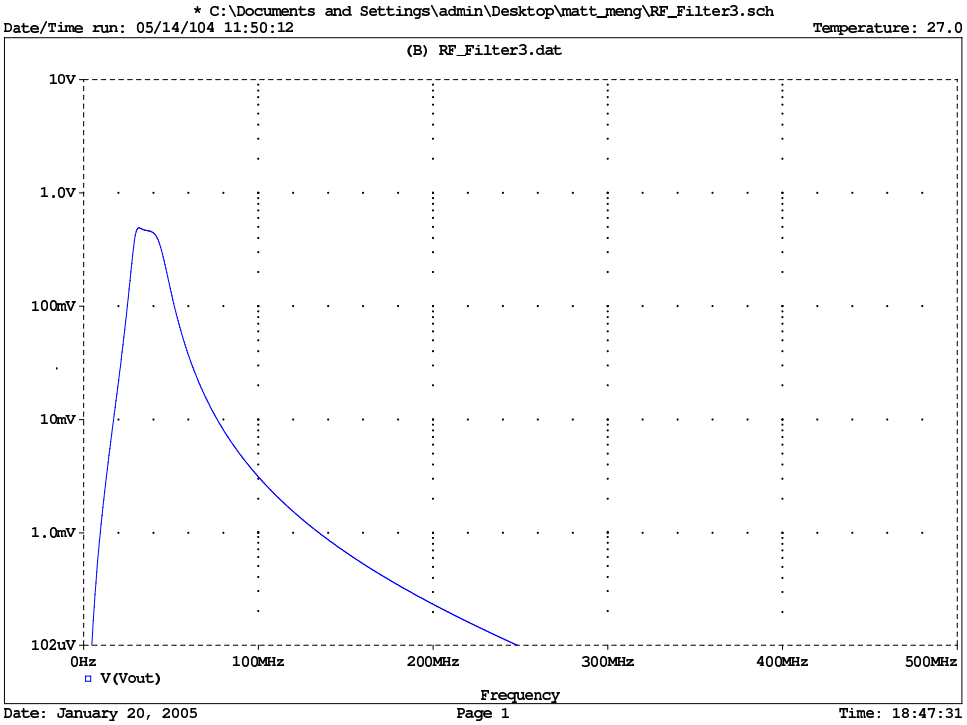

Figure 4.6: RF filter model SPICE sweep, $|V_{in}| = 1.0$ [volts]

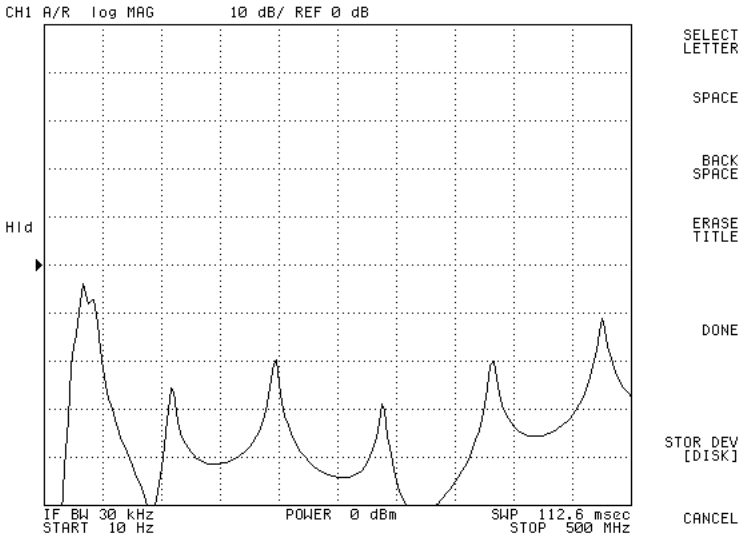

Figure 4.7: Filter transfer function measurement on the network analyzer

Chapter 5

Circuit for Detection of Broadband Emissions

Another way to sense the current or voltage behavior in the arcing conductor is to use an antenna placed close to the conductor. Excitation due to arcing will couple to the antenna, and signals from the antenna can be used for the purposes of detection.

5.1 RF Current Detector Board

Our detection strategy is to detect several isolated frequencies or sweep over a range of frequencies. Spectral content tells us that arcing is present, and checking over a range of frequencies helps ensure that we are not being fooled by spurious external transmissions in a specific and isolated frequency range.

Figure 5.1 is the main circuit schematic for the current based detector board. There are four main stages to consider. The input stage consists of the input signal coming from our antenna sensor and a buffer to maintain that signal. Next, because the input is broadband noise, we want to select specific frequency content using a filter stage. To detect how much power there is in our filtered signal we have a power detection stage. The power detection stage will output a DC voltage to indicate how much power passes through the filter. We then take this DC voltage and indicate it visually using an LED meter, or use it as a trigger for a mitigation device. A more detailed description of the operation of the circuit follows.

5.1.1 Buffer

Because we are working with very small signals and a sensor which is sensitive to loading, the first task necessary in designing an analog detector circuit is to buffer the input.

5.1.1.1 Estimation of Arc Output Impedance

When designing the input stage to our detector, it is useful to develop a circuit model for an arc. A circuit model has the additional utility of describing arc behavior over a wide range of operating conditions.

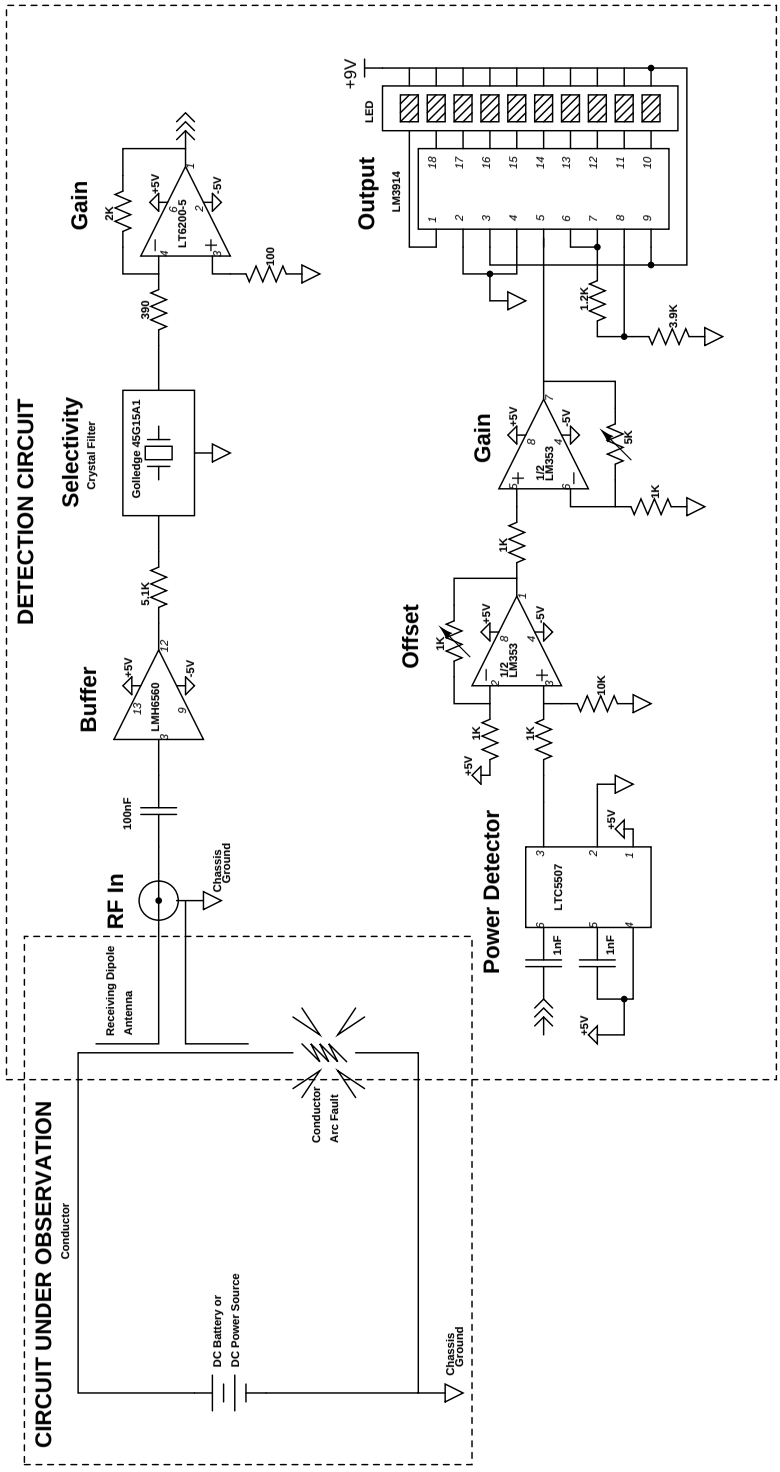

Figure 5.1: Main detector circuit schematic

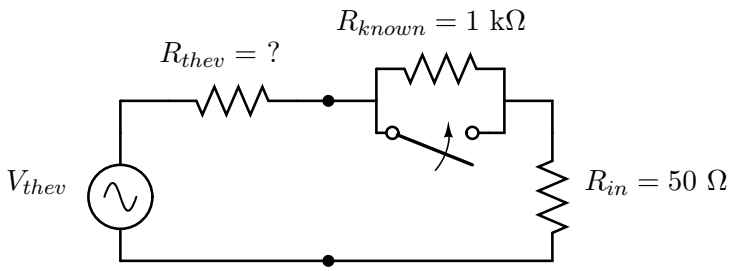

Figure 5.2: Method for estimating output impedance of an arc

We will use a Thevenin equivalent circuit as our circuit model. Because arcing signals are random and chaotic, there are an infinite number of time dependent Thevenin sources and equivalent impedances, each representing a distinct broadband frequency. It will not be possible to determine these sources or impedances exactly. We can however perform tests to give us useful approximations for the equivalent output impedances of an arc.

Figure 5.2 shows a circuit schematic depicting the measurement procedure used for estimating the Thevenin equivalent output resistance. The voltage source and unknown resistance represent the Thevenin equivalent model for a given frequency. The 50Ω resistance is the input impedance to the spectrum analyzer. If we connect the arcing voltage to the spectrum analyzer using a cable much shorter than the wavelengths we are observing, we can assume there are no transmission line wave reflections, and that the input impedance of the spectrum analyzer forms a divider with the Thevenin equivalent output impedances.

Artificially increasing the output resistance of the Thevenin circuit by adding a resistor allows us to estimate the magnitude of that unknown output resistance R_{thev}. Theoretically, any measurable change in the divider voltage will allow us to calculate this unknown. However, because the measured divider voltage is quite noisy, we will try to make this change in divider voltage large with respect to the noise. In order to significantly change the divider's output voltage, the added resistance cannot be small compared to the unknown output resistance. If we know the value of the added resistance, and can measure the output voltage (or power), it is straightforward to determine the equivalent output resistance.

We took sample measurements with and without the added resistor. One measurement without the added resistor measured -45 dBm input power into the spectrum analyzer at close to 35 MHz. With the resistor, the input power decreased to -61 dBm. This brings us to the following input power equations

$$\begin{aligned} \text{Without } 1k\Omega\text{:} \quad & \frac{V_{thev}^2 \cdot \left(\frac{50}{R_{thev}+50}\right)^2}{50} &= 10^{\frac{-45}{10}}[\text{mW}]\ (-45[\text{dBm}]) \\ \text{With } 1k\Omega\text{:} \quad & \frac{V_{thev}^2 \cdot \left(\frac{50}{R_{thev}+1000+50}\right)^2}{50} &= 10^{\frac{-61}{10}}[\text{mW}]\ (-61[\text{dBm}]) \end{aligned} \tag{5.1}$$

The comparison is approximate because the voltage source is not exactly the same in each measurement. However, because the measurements do not vary drastically among trials, we can make the simplifying assumption that the voltage source is ideal and constant. As such, the power ratio is then

$$\frac{(R_{thev}+1000+50)^2}{(R_{thev}+50)^2} = \frac{10^{\frac{-45}{10}}[\text{mW}]}{10^{\frac{-61}{10}}[\text{mW}]} \approx 40 \tag{5.2}$$

Solving for R_{thev}, we calculate $R_{thev} \simeq 138\Omega$, (at 35 MHz). Using different measurements, this value can change slightly. Mainly we are interested in the order of magnitude of this output impedance so that when we develop a detection circuit, we have an idea of how to choose a buffer with a suitable input impedance.

5.1.1.2 Buffer Integrated Circuit

It is possible to build buffers and amplifiers using transistor based circuits, but because we are working with fairly high frequencies we found that the best approach to take was to use high speed buffers and operational amplifiers available to us as integrated circuits (IC's).

One such buffer we found was the LMH6560 quad, high speed, closed loop buffer. To test this buffer, we were able to obtain an IC evaluation printed circuit board from National Semiconductor (NS Part CLC730145). This evaluation board was extremely useful in a way outside of testing the buffer; it gave us insight into the proper printed circuit board design techniques necessary at these frequencies. Specifically, we duplicated the proper use of a ground plane, trace layout techniques, power rail design, and bypassing techniques when laying out our arc detector board.

The input resistance of this buffer is specified with a typical value of $100k\Omega$. In parallel with this is a 2 pF input capacitance, which dominates at high frequencies. Because this input capacitance is quite small, we will still have enough input impedance to ensure that the buffer stage does not load the arcing signal, as analyzed in the previous section.

5.1.2 Selectivity Filter

We will use simple bandpass filtering to process the broadband signal input. The filter should select a fairly narrow band from the broadband signal present at the input. If the bandwidth of the filter is too large, it will be hard to distinguish wanted signals from spurious inputs; strong selectivity helps us prevent false-positive detections.

It should be noted however, that an accurate detector would require a better filtering scheme. No matter what the center frequency or bandwidth, the selectivity scheme could be compromised by a spurious signal from a transmission tower, amateur radio device, or similar. To avoid this, a detector could check multiple distinct frequency ranges, or a sweep over one or more frequency ranges. For the former, logical AND gates would be suitable for an analog electronic implementation. For the latter, a common approach used in amateur radio is to use a "Varicap" diode. This element is a voltage-controlled capacitor, and can be used for tuned filtering. Digitally tuned radios often use this exact method for frequency selection.

5.1.2.1 Active Filter Design

For selectivity we designed an active filter using a parallel resonant LC tank circuit, as shown in Figure B.2. We encountered difficulties when we tried building this filter. After applying feedback analysis, we understood why this design would not work. An explanation of these problems is included in Appendix B.

As a workaround, it is possible to use a resonant tank circuit in a passive filter configuration. Such configurations however, do not provide a sufficiently narrow bandwidth necessary for our application. Because of this, we investigated the use of crystal filter packages to replace our own active network.

We obtained high Q sample filters from the filter supplier Golledge Electronics. These components use piezoelectric effects to couple the electrical inputs and outputs to internal quartz wafers, employing their mechanical resonance for filtering. Using a 45.0 MHz center frequency, 15 kHz pass band (part no. 45G15A1) we were able to filter the input signals with the tight selection we were aiming for. A picture of these filters is shown in Figure 5.3. Specifications for the components can be obtained directly from Golledge [7].

Because the filter is used in an open loop configuration, it does not suffer the same complications as the active filter, described in Appendix B.

5.1.3 Power Detection Stage

One way to build a power detector is to use a diode and a capacitor in peak detector configuration as shown in Figure 5.4. When the input signal is greater than the DC voltage

Figure 5.3: Photograph of Golledge crystal filters

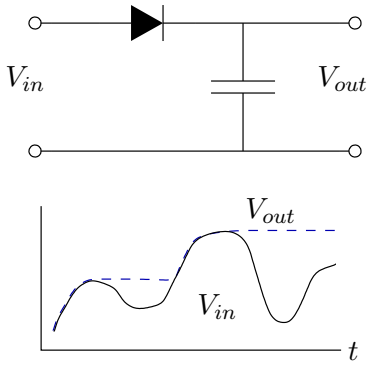

Figure 5.4: Diode and capacitor peak detector

level of the capacitor, current is injected into the capacitor thereby raising its DC voltage. The magnitude of this voltage is related to the power delivered from the previous circuit stage.

We found an RF Power Detection IC (Linear Technology, LTC5507) which essentially performs this same function. The capacitor is an external component selected according to the LTC5507 data sheet. This chip was readily available to us because of its common use in cellular telephone applications; the same function is performed by cell phones in detecting antenna signal strength.

The first page of the LTC5507 datasheet (see Appendix C) shows a plot titled "Typical Detector Characteristics". It shows the nonlinear curve relating the RF input power to the DC output voltage. With less than -22 dBm input power, the curve is fairly flat and the device outputs a constant .125 volts. Above -22 dBm input power, the DC level increases until 14 dBm (1.1 volts), the maximum rated input for the device. These specifications allow us to suitably design the preceding gain stage to take advantage of the power detector's full output range. As shown in the main schematic, we amplified the filter output by $2000 \div 390 = 5.1$.

5.1.4 Signal Level Readout

Depending on the strength of the input signal, the LTC5507 will output a DC Voltage between .125 and 1.1 volts. Using this, we can light up an LED display to indicate the strength of the signal passing the filter. We do this by using an LM3914 LED Display driver, which when configured as in the application note for the device, will turn on between 0 and 10 LED's as the input level varies between 0 and 5 V DC. By conditioning the LTC5507 output voltage using offset and gain stages, we can make the display turn on fully lit LED's when the signal strength is greatest.

Because the power detector outputs DC, we can do the offsetting and gaining using standard DIP package opamps. By using potentiometers we can freely adjust the offset and gain.

5.1.5 Power Supply

Power for integrated circuits is supplied using two nine volt batteries, a positive 5 volt regulator (7805), and a negative 5 volt regulator (7905). The power lines used on the board are ± 5 volts, +9 volts, and a common ground.

A ten volt zener diode (1N758A) is used across the ± 5 volt rails in a clipping configuration. Any increase above the ten volt reverse breakdown causes the zener current to jump and the zener voltage to stay pegged at 10 volts. This is used to provide over-voltage protection for the integrated circuits.

5.1.6 Board Design and Layout

For the input RF connector and ground lead, we used screw terminals in conjunction with pads of exposed tinned copper (sans solder mask). The screw terminals compress the antenna and ground leads against these pads to produce reliable, removable connections.

To avoid parasitics, specifically series trace inductances, it is best to take special precautions when designing a board layout. First, traces carrying RF signals should be kept very short, as well as the traces powering integrated circuits processing those signals. This will correspond to a compact layout. The final dimensions of the board were 3652 mils (thousandths of an inch) by 2152 mils, or about 9.3 cm by 5.5 cm. The portion of real estate devoted to RF signal processing is considerably smaller than this.

Second, we use a ground plane under the entire circuit. This makes a two layer layout more difficult because all signal and power traces must be run on one side of a board. Where it is necessary for two traces to cross paths, a small area of the ground plane is cleared and an underpass is formed by means of two vias.

Finally, we liberally used capacitive bypassing, both close to the power regulators, and at

the integrated circuits. This keeps power lines clean by shunting high frequency noise to ground.

The board was designed using Eagle CAD Software. We sent the board to Advanced Circuits, Inc., for manufacturing. After mounting components, were were able to successfully use the detector. A discussion of these results is found in Chapter 7.

Chapter 6

Sensing Methods

In our original investigations on frequency based arc detection, we began by examining the properties of arcing voltage. We successfully built and demonstrated a voltage based arc detector as a proof of concept for broadband emissions detection.

Arcing voltage, however, is not an accessible parameter away from the test bench. Specifically, we connected the voltage based arc detector in parallel with the arc gap. Because it is impossible to predict where a failure will happen along the length of a conductor in a real life harness, it is difficult to make this kind of voltage based measurement of arcing phenomena.

Techniques based on current measurements however, are not subject to this difficulty. Currents in the arcing conductor will be the same as or related to the currents passing through the arc itself. We can therefore effectively monitor for arcs by examining the currents in associated conductors.

This chapter describes some of the possible techniques for sensing arcing currents.

6.1 Current Clamp Sensors

There are several types of prefabricated current sensors which one might consider for our application.

6.1.1 LEM Sensors

LEM sensors, named after the company which sells them (short for Liaisons Electroniques-Mecaniques), or similar sensors are one possibility. LEM sensors are classified into two main categories; open loop and closed loop.

Both employ Hall devices to sense magnetic fields produced by currents in the conductor under test. A good description of how Hall devices work is available from Honeywell Incorporated [3].

Open loop LEMs use the Hall sensor and a differential amplifier to produce a facsimile output current as shown in Figure 6.3. Closed loop LEMs use this output to drive a push pull current amplifier connected to a coil around the magnetic circuit as shown in Figure 6.4.

Figure 6.1: Current clamp from Solar Electronics

Figure 6.2: LEM Current Sensors

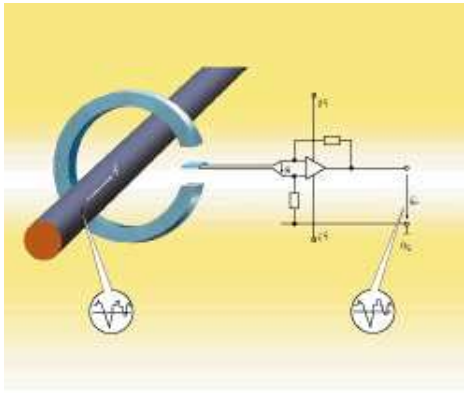

Figure 6.3: Open loop LEM sensor diagram

The polarity of this connection is such that mirrored currents in the coil produce fields which cancel those of the primary. The advantages of the closed loop configurations are those of normal feedback systems: resilience to environmental changes, improved bandwidth, and overcoming the nonlinear effects of the magnetic circuit.

Unfortunately, LEMs were not suitable for our needs. According to the product literature available from LEM, the fastest available sensors in this category are too slow for our purposes, with bandwidths of 500 kHz. This is not a limitation of the electronics and amplifiers of LEM devices, but rather the nature of the magnetics used to focus magnetic flux on the Hall device. Because we are interested in measuring much faster currents, in the tens of megahertz range as discussed in Chapter 4, we cannot use LEMs for current sensing.

6.1.2 High Frequency Current Probes

Another type of current probe which is not limited by the frequency constraints of LEM devices are high frequency clamp-on or fixed-window transformer type current probes such as those available from companies such as Eaton, Stoddart, or Solar Electronics. These devices are designed to work into the hundreds of megahertz. They usually have N-type output connectors, intended for use with 50 Ohm RF receivers or spectrum analyzers. While we are not certain how the devices are constructed, the product literature denotes them as "inserted primary toroidal transformers".

We had a few Solar Electronics probes available for testing in our lab (Solar Parts 9260-1N & 9320-1N). These probes were specified to function up to 200 MHz. We soon discovered that the probes were not good at measuring arcing currents. In particular, when we clamped the probe around an arcing conductor, the input power displayed on the spectrum analyzer was not significantly greater than the noise floor of the instrument for any given frequency.

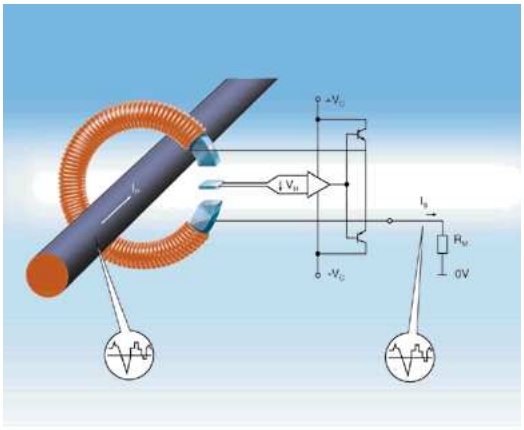

Figure 6.4: Closed loop LEM sensor diagram

According to the probe manuals, the probe will not heavily load the conductor under test (when compared with arcing source impedances as discussed in Section 5.1.1).

Because these probes are built for high current measurements ($\tilde{3}00$ amps RMS current maximum), we speculated that there may be a non-linearity which makes the probe not suitable for the small amplitude currents we were trying to measure. Because it was apparent that the probes were not suitable for this purpose, we did not pursue this issue further. It may have been helpful to characterize these probes by using known test currents (as opposed to chaotic arcing ones) to study any non-linearities which may be present.

6.2 Rogowski Coils and Resonant Sensing

Another way to measure these currents is to use Rogowski coils. Rogowski coils are windings wound of plastic or air cores, usually used in a transformer configuration. Because there is no iron or ferrite core which would saturate with a high DC field, Rogowski coils are suitable to the arcing application, where we are trying to measure small alternating currents on top of large direct currents.

Using magnet wire rolled around the threaded end of a bolt, a 25 turn monolithic linear inductor coil was fabricated. After removing the coil from the bolt, it was bent this around the single turn of the primary conductor to attain the toroidal configuration shown in Figure 6.5. To the left of the magnet wire secondary are two similar attempts at Rogowski coil construction using series connected air-core chip inductors.

We were unsuccessful with a few configurations of Rogowski coils. While we pursued some analysis to understand why, we encountered measurement difficulties which did not quickly

Figure 6.5: Photograph of constructed Rogowski coils

lead to an analytical explanation. Although Rogowski coils may still have potential as broadband emissions sensors, we did not use them.

6.3 Antenna Sensor

An alternative to the previous sensing techniques is to use a small wire which would act as an antenna, placed close to the conductor exhibiting broadband emissions. Excitation due to arcing will couple to the antenna via electric or magnetic fields, and signals from the antenna can be used for the purposes of detection. We had good success with these sensors, as compared with the sensors discussed in the previous sections.

It is possible to use standard round wire or flat wire. The flat wire offers a few advantages over its round counterpart. Because of its shape and stiffness, it holds better to the conductor under test. Additionally, we expect a higher capacitance between a conductor and flat wire antenna because of its larger surface area. This higher capacitance may provide for more signal coupling to the antenna. We performed our tests with American Wire Gauge (AWG) 16 flat magnet wire.

A more rigorous analysis of this type of sensor may serve to improve its qualities for broadband emissions applications. For most of our tests, we used antennas which were 20 centimeters long (with an additional 5 centimeters which extended radial from the arcing conductor to the detector circuit as visible in Figure 7.3). We tried a few simple variations on this antenna length (10 centimeters long and 40 centimeters long, each with similar 5 centimeter extensions), but found no great difference in the amount of signal picked up.

Chapter 7

Detection Circuit Results

To test the arc detector, we built a test bench simulating an arcing car harness in our lab. This allowed us to use laboratory equipment to debug circuits and take measurements. The first section of this chapter discusses the test bench, and the subsequent two sections cover tests performed on it. Additionally, we used the detector in a 1997 Toyota Corolla, described in the final section of the chapter.

7.1 Experiment Test Bench

A schematic depicting the test bench is shown in Figure 7.1. Three car batteries connected in series provide DC power for the arcing source. A sheet of brass is used to simulate the car chassis, and an insulated, heavy gauge conductor represents the harness under test. This stranded conductor is 220 centimeters long, 5.5 millimeters in diameter (not including insulation), and is bent in a zig-zag fashion to conserve horizontal bench space. Two 1.0 ohm resistors provide current limiting as discussed in section 4.2.

In series with the arc gap are two switches, S_A and S_B. S_A is a normally closed emergency stop switch, used to extinguish arcs. S_B is a large blade switch used to break the circuit when no tests are being performed.

Points 1, 2, 3 and 4 are connections to the brass ground plane. As in a car chassis, the return path for arcing currents is provided by the ground plane.

The arc gap is a broadband signal source. For experimentation, this source can be replaced by a function generator as illustrated in Figure 7.1. For protection from the large DC arcing voltage, a large electrolytic blocking capacitor C_{big} is used. To prevent high onrush currents, the capacitor should be charged to the battery voltage before the function generator is connected to the circuit.

Finally, an oscilloscope and RF measurement probe (Probe Master Inc., model 4251 as shown in Figure 7.2) are used to measure the power detector input voltage on the detection board. While the LED meter output gives us an approximate, quantized indication of how much signal pickup is passing the input filter, the probe allows us to measure exact amplitudes. Because we are working with RF, it is important to use special probes which do not load down these signals.

Typical measurement procedure begins by closing all switches, turning on the detector

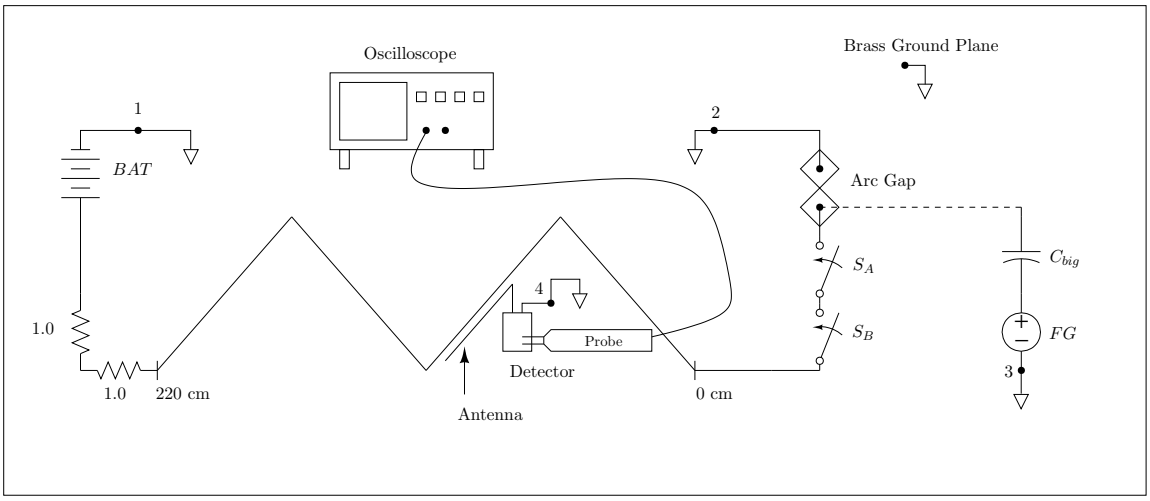

Figure 7.1: Schematic of experimental test bench

Figure 7.2: Probe Master 4251 RF measurement probe

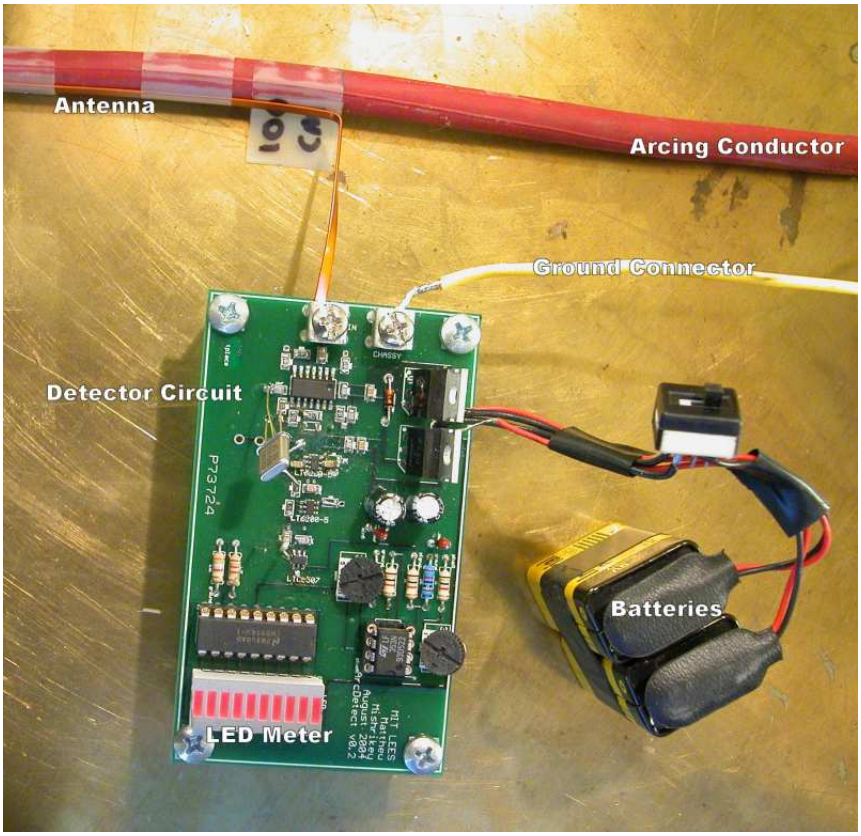

Figure 7.3: Photograph of detector circuit on test bench

circuit, and then initiating or simulating an arc. During arcing, the LED meter will indicate the filtered arcing power.

A closeup photograph of the detector circuit as arranged on the test bench is shown in Figure 7.3.

7.2 Distance from Arcing Source Tests

One question to pursue is whether the detector's position along the harness with respect to the arcing source affects its ability to detect. That is, if the arc occurs far away from the detector, can we still detect? To understand this better, we tried an experiment which we later realized was not entirely relevant, but nonetheless insightful.

First, we taped several identical antennas at various positions along the conductor. We could then easily move the detector and measurement apparatus to different positions along the harness. To understand this proximity effect, we would simply measure signal strength

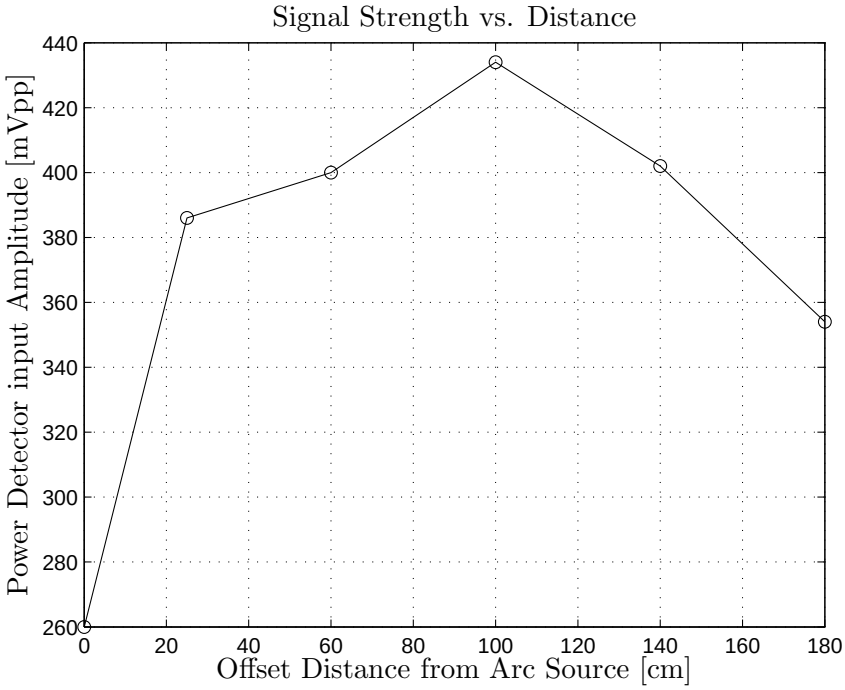

Figure 7.4: Graph of signal strength vs. distance along conductor

versus position.

We decided in advance that the arc source is not suitable for this type of experiment because it is different from trial to trial. The arc itself is chaotic, and arc currents have a time varying, non-predictable frequency spectrum. Thus, even when the position variable is held constant, signals measured from the detector will vary from moment to moment, and from trial to trial.

If however, we simulated the arc by using a constant signal source as described above, we would be able to perform the experiment with all variables constant, except position.

The results of this experiment are shown in Figure 7.4. We see that as we start to move away from the arcing source, the received signal strength increases until a maximum near 100 cm, beyond which the signal strength decreases. Because of this behavior, it is reasonable to speculate that we are measuring a voltage standing wave pattern (VSWP). A complete cycle of VSWP would correspond to a half wavelength. We did not measure a complete cycle because we were limited by the conductor length of 220 cm. The pattern measured appears to represent slightly more than a quarter wavelength. This is in agreement with the frequency we used. The function generator was set to the filter frequency of 45 MHz, which corresponds to a wavelength of 6.67 meters. A quarter wavelength is then 1.67 meters.

Beyond being a good exercise in measuring transmission line standing wave patterns, and

confirming our measurement technique, this experiment gave additional insight. The periodic variations in amplitude occur because we are exciting the transmission line with a constant amplitude sinusoid. Because arcing does not resemble this type of excitation, no sinusoidal steady state is achieved, and no standing wave variations will exist. Accordingly, signal strength should not vary as a function of distance.

When we repeated these tests using the detector LED meter as a qualitative approximation of arcing signal strength, we found equal signal strength at all positions along the conductor.

7.3 Car Tests

In keeping with the discussion on SAE specifications of section 4.3.2, we tested the detector on a conventional 12 volt car harness. Specifically, we are interested in possible false positive detections. This is not an entirely fair assessment as to whether the detection system will or will not fail in a 42 volt vehicle; both systems are subject to separate electrical noise and noise requirements. This is still a useful exercise because it studies the behavior of electrical components which could be common to both systems.

An antenna was taped to the conductor connecting to the positive battery terminal of a 1997 Toyota Corolla. The position of the antenna, approximately 30 cm along the conductor away from the battery terminal, was dictated by the geometry of the harness and engine compartment. In particular, we needed a fairly straight 20 cm of harness cable to facilitate the attachment of the antenna, as well as a secure place to attach the detector.

7.3.1 Tests with Engine Off

The detector was activated with the engine off, and several loads were tested for interaction with the detector.

Neither pulsed on-off actuation of power windows, nor continuous operation of up to four windows registered on the detector's LED meter. Windshield wipers, on any setting (intermittent, low, medium and high) did not register on the detector output. Radio operation, including on-off toggle, frequency scanning, and high volume radio play had no effect. Brake actuation in the stationary vehicle did not have an effect. Operation of headlights, high-beams, turn indicators, and hazard signals did not have an effect.

Electronic power door lock operation was able to make the first unlit bar of the LED meter flicker. When compared to stable arcing, the flicker signifies a much smaller amplitude signal, lasting for a much shorter duration. This result is also dwarfed by the LED meter output triggered by unstable sparking, which causes several LED bars to flicker with greater brightness (corresponding to a longer excitation).

7.3.2 Tests with Engine Running

With the car engine running, we were able to notice a more significant, repetitive flicker on the detector output. This behavior is noticeably different from the detector output during an arc event. Arcing causes the LED meter to almost entirely and brightly light up, with the top two or three bars toggling on and off as the received signal fluctuates. The noisy engine flicker, on the other hand, is dim and fleeting in comparison.

This was not a surprising result, as we expected some excitation due to pulse width modulating (PWM) circuits, and possibly from loads like the ignition system, which repetitively draw impulses of current. We did not determine exactly which loads contributed to the detector's excitation. We can however, based on these observations, categorically separate these disturbances from the noise caused by arc events.

The easiest way to make this distinction in analog is to add a low pass filter immediately after the power detector chip of the detection circuit. This would allow the relatively constant arc event output to pass on to the LED meter, and block the fluctuations caused by engine related noises. While we did not implement this feature into our circuit, it is visually apparent that a low pass filter would separate the different types of noise.

Finally, with the engine running, we repeated the tests on windows, wipers, radio, brakes, lights and door-locks. With the door-locks, we found the same flickering of the first unlit bar of the LED meter, on top of the background "engine flicker" noise. With all other loads, we found no additional response on top of the background noise. In the case of door-locks, a properly designed low pass filter would suitably attenuate the flicker of the first LED meter bar, in addition to the noise caused while the engine is running.

In summary, the tests performed in the car confirmed our understanding of noise disturbances in the car, as well as the operation of our detector. They suggest that use of our detector may be a feasible solution for arcing, and also suggested an improvement to the detector in response to step or impulse current transients in the car.

Chapter 8

Conclusions

The goal of this research was to invent a reliable detection strategy to solve the problem of DC electric arcing. A variety of possible methods are available in published papers, conference proceedings and patents as discussed in Chapter 2. Still, there is no established method for detection, there are no commercial solutions available at this time, and arcing remains an unsolved problem for the automotive industry.

This research was performed under the auspices of the MIT/Industry Consortium on Advanced Automotive Electrical/Electronic Components and Systems Solution. Though we had the automotive application in mind, our results extend to DC arc detection in non-automotive domains.

8.1 Summary of Results

We began by investigating phase noise and broadband emissions as possible indicators of DC arcing. Our initial findings were that phase noise is not a good metric for detecting arcs, but that broadband emissions are.

Broadband spectral measurements of arcing signals were taken, and calculations based on noise emissions standards showed that even current limited arcs produce extensive broadband noise.

These results led to the development and testing of a functional arc detector. This type of detection has many positive traits. First, the detector is non-invasive; no already installed harness wiring or car circuitry needs to be modified to install the detection system. Detectors can be conveniently placed and do not require line of sight or sound to the arc. It can equally detect series and parallel arc faults, unlike other differential measurement systems. Likewise, detection is not limited to a defined protection zone; it can detect arcs happening anywhere along a contiguous harness in which arcing broadband emissions are readily conducted. Finally, detection is fast, and reliable.

Several sensing methods were investigated, leading to the successful use of a simple wire antenna for picking up broadband emissions.

A simulated car harness test bench was built, allowing us to conduct investigations using our prototype detector. We found that the location of the antenna and detector along the harness does not significantly affect the amount of arcing emissions picked up. Also, after

placing the detector in a 12 volt car, we learned how to improve our detector to filter out spurious excitation. At the same time, we learned that most normal loads will not trigger false positive detections.

8.2 Recommendations for future work

A plausible proof-of-concept detector has been successfully implemented and presented. As outlined in Chapter 4, the input filtering method is simple and should be made more elaborate to prevent false-positive detections. This could be done by monitoring several distinct narrow bands, or by sweeping frequency ranges. Alternatively, a more mature and robust method is recommended in [4].

The problem of localization still needs to be solved. At a minimum, one needs to know which harness branch or subcircuit has been affected. Ideally, a detection system will determine the exact position of a fault. Acoustic detection offers the possibility of localization by triangulation, as discussed in [8]. Because electromagnetic waves travel much faster than sound waves, triangulation using multiple broadband emissions detectors would require very sensitive timing measurements. Additionally, an optimal number of detectors would need to be considered.

Finally, research should be performed to propose a suitable mitigation strategy in the event arcing is detected. Opening circuits with breakers may not be an adequate approach given ever-increasing safety critical load such as “steer-by-wire” and “brake-by-wire”. Redundant cabling may be necessary in these particular cases. Cases in which multiple simultaneous cable faults occur should be considered.

Appendix A

Index of Related Patent Material

Duplicate patent titles with different patent numbers indicate patents which have been updated with corrections.

U.S. Patent No.	Patent Title
4466071	High impedance fault detection apparatus and method
4967158	Portable detector device for detecting partial electrical discharge in live voltage distribution cables and/or equipment
5083086	Differential Arc Reflectometry
5142234	Particle beam accelerator electromagnetic arc detection system
5164662	Detection of radio frequency emissions
5185684	Frequency selective arc detection
5268644	Fault detection and isolation in harness by TDR
5352984	Fault and splice finding system and method
5373241	Electric arc and radio frequency spectrum detection
5477150	Electric arc and radio frequency spectrum detection
5481195	Method for finding a fault on an electrical transmission line
5530360	Apparatus and method for diagnosing Faults
5608328	Method and apparatus for pinpointing faults in electric power lines
5706159	Circuit interrupter including an electric arc monitoring circuit
5729145	Method and apparatus for detecting arcing in AC power systems by monitoring high frequency noise
5986860	Zone arc fault detection
6088205	Arc fault detector with circuit interrupter
6094043	Arc detection sensor utilizing discrete inductors
6246556	Electrical fault detection system
6377055	Arc fault detector device with two stage arc sensing
6407893	Arc fault detector with circuit interrupter and early arc fault detection
6421214	Arc fault or ground fault detector with self-test feature
6577138	Apparatus for detecting arcing and overcurrents in DC electrical systems subject to cyclic disturbances
6625550	Arc fault detection for aircraft

listing continued on page 50

U.S. Patent No.	Patent Title
	continued from page 49
6639769	Arc fault detector with circuit interrupter
6667691	Apparatus for the detection and early warning of electrical arcing fault
6683766	DC arc detection and prevention circuit and method
6736944	Apparatus and method for arc detection
6751528	Residential circuit arc detection
6777953	Parallel arc fault diagnostic for aircraft wiring
6781381	Electric arc synthesis for arc detector testing and method for arc testing
6782329	Detection of arcing faults using bifurcated wiring system
6785104	Low energy pulsing device and method for electrical system arc detection
6798211	Power line fault detector and analyzer
6809483	Method and apparatus for arc detection and protection for electronic ballasts
6810069	Electrical arc furnace protection system

Appendix B

Feedback Analysis of Active Filter

This section contains a discussion of a filter design which did not work. We document this here for completeness, and to show some of the complexities involved with designing active filters.

We designed a parallel LC resonant tank circuit to perform the filtering at a frequency within the range of interest. The center frequency of this resonator is determined by $f_0[Hz] = \frac{1}{2\pi\sqrt{LC}}$. Because of equivalent series resistance in the windings of the inductor and leads of the capacitor, the magnitude of the total parallel impedance will not be infinite. The impedance of the network is

$$\begin{aligned} Z_T &= Ls \parallel \frac{1}{Cs} \parallel R_T \\ &= \frac{Ls}{LCs^2+1} \parallel R_T \\ &= \frac{\frac{LR_Ts}{LCs^2+1}}{\frac{Ls}{LCs^2+1} + R_T} \\ &= \frac{Ls}{LCs^2 + \frac{L}{R_T}s + 1} \end{aligned} \tag{B.1}$$

We can experimentally characterize the behavior of the tank circuit by testing it with an impedance analyzer. Figure B.1 shows the impedance of the tank circuit between 100 kHz and 500 MHz. The top subplot shows the magnitude of the impedance, ranging from a minumum of 200 mΩ to a maximum of 100 kΩ. The bottom sublot shows the corresponding phase. The plot window has a vertical range of 360 degrees, and the phase of the impedance of the network varies between minus 90 and plus 90 degrees. The impedance analyzer (Agilent 4395A) is able to fit the resulting data and determine component values for an equivalent RLC circuit. The marker displays a peak impedance of 12.3 kΩ at 38.2 MHz.

Using this impedance, we designed an active filter as shown in Figure B.2. This is an inverting gain configuration with the tank circuit replacing a resistor as the feedback element. At frequencies far from the center frequency of the tank circuit, the tank circuit is essentially a short circuit and the gain of the filter is minute. At the center frequency, the gain magnitude should be the ratio of the magnitude of the feedback impedance to the input resistance, in this case approximately 3.

Because of the high frequencies we are working with, we need a fast device for the active filter's op-amp. The LT6200-5 is has an 800 MHz gain bandwidth product. If we are conservative and say the maximum gain is 3, we will be allowed a bandwidth of $800MHz \div 3 = 267MHz$, well beyond our requirements.

Simulating this selectivity stage using PSPICE confirmed the theory of operation for the active filter.

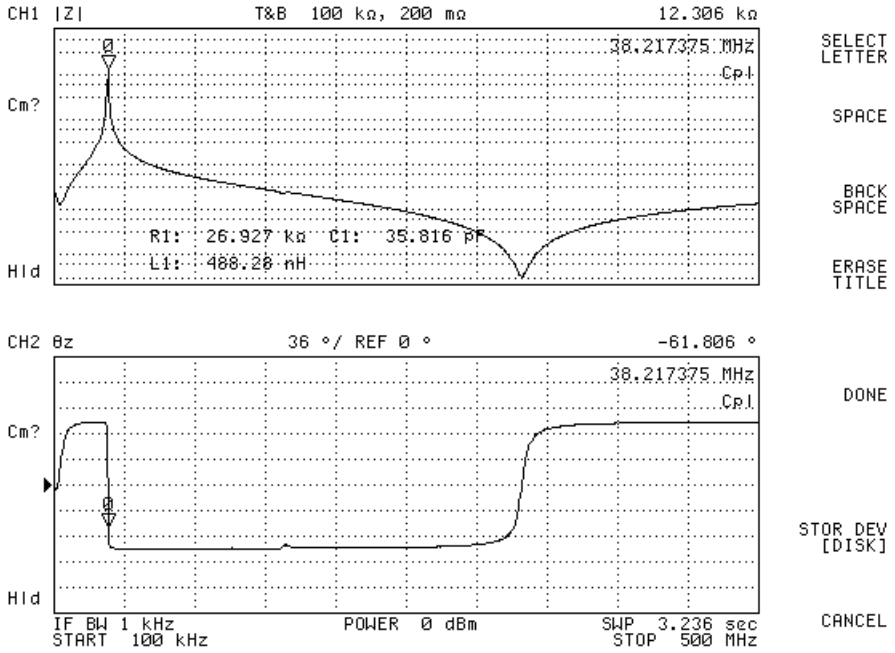

Figure B.1: Impedance analyzer sweep of LC tank circuit

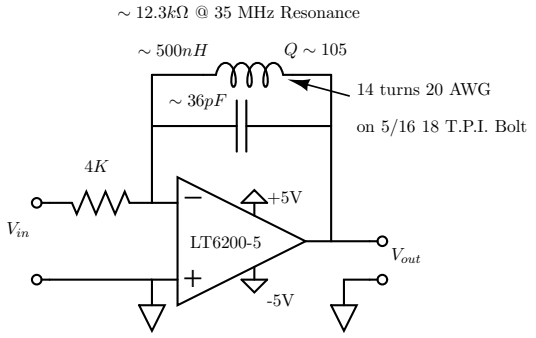

Figure B.2: Attempted active filter design using LC tank circuit in feedback path

We use a model of the device downloaded from the National Semiconductor website, and component values from the impedance analyzer fit. A complete netlist follows, and the corresponding probe output is shown in Figure B.6.

```
*Selection Filter for ARC Detection*
.include LT6200-5.lib
***ELEMENTS
Xamp24601 inpos inneg vplus vminus out shdn LT6200-5

Lfil inneg out 488.28E-9
Cfil inneg out 35.816E-12
Rfil inneg out 26.927E3

Rin in inneg 4K
Roffset inpos 0 4U
Rpullup vplus shdn 4U

Vpos vplus 0 DC 5
Vneg 0 vminus DC 5
Vac in 0 AC .1

***CONTROL STATEMENTS
.AC DEC 100 500E3 100E6
*100 points per decade

***OUTPUT STATEMENTS
.PLOT AC VDB([out]) VP([out])
.PROBE V([out])
.END
```

Feedback analysis of filter

Despite our circuit simulation and theory of operation, we discovered that the circuit is unstable and oscillates at a frequency limited by the slew rate of the op-amp, as shown in Figure B.3. The vertical cursors show the resulting triangle wave to have a frequency of 30.5 MHz. The vertical scaling is 1.0 volts per division, and the time scaling is 20 nanoseconds per division. To understand why this oscillation occurs, we performed a feedback analysis of the circuit.

Labeling the input and feedback impedances as Z_1 and Z_2 respectively, we can write the following equations.

$$V_{out} = -A(s)V_{in} \tag{B.2}$$

$$V_m = \left(\frac{Z_2}{Z_1 + Z_2}\right) V_{in} + \left(\frac{Z_1}{Z_1 + Z_2}\right) V_{out} \tag{B.3}$$

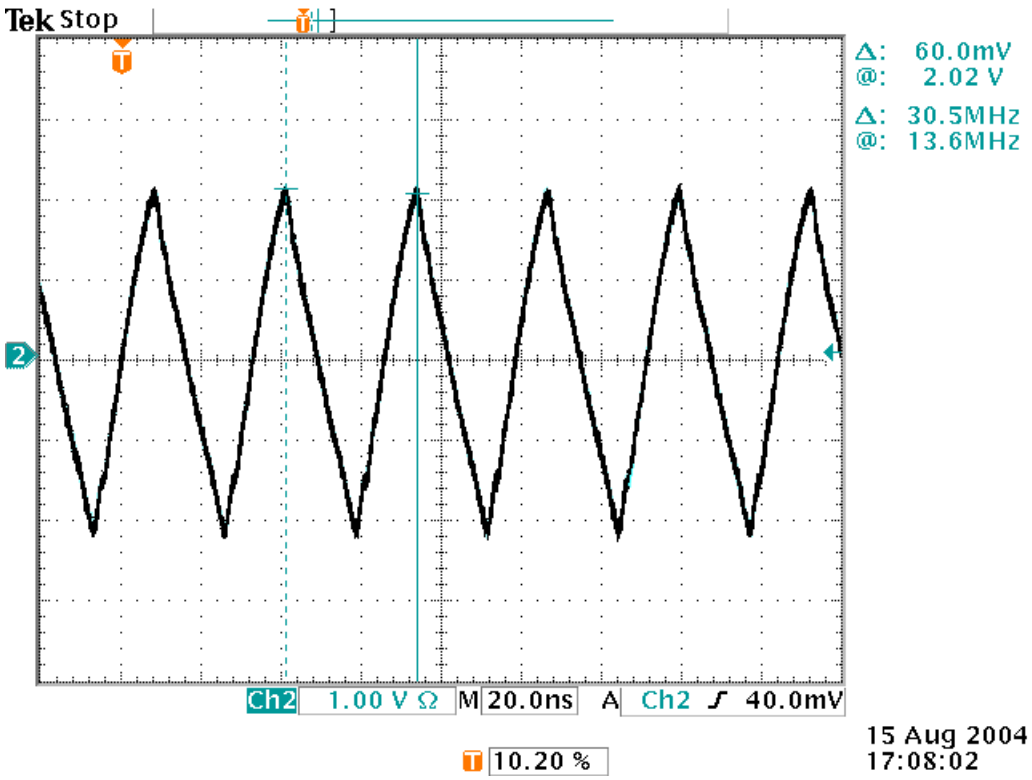

Figure B.3: Slew limited oscillation of active filter circuit

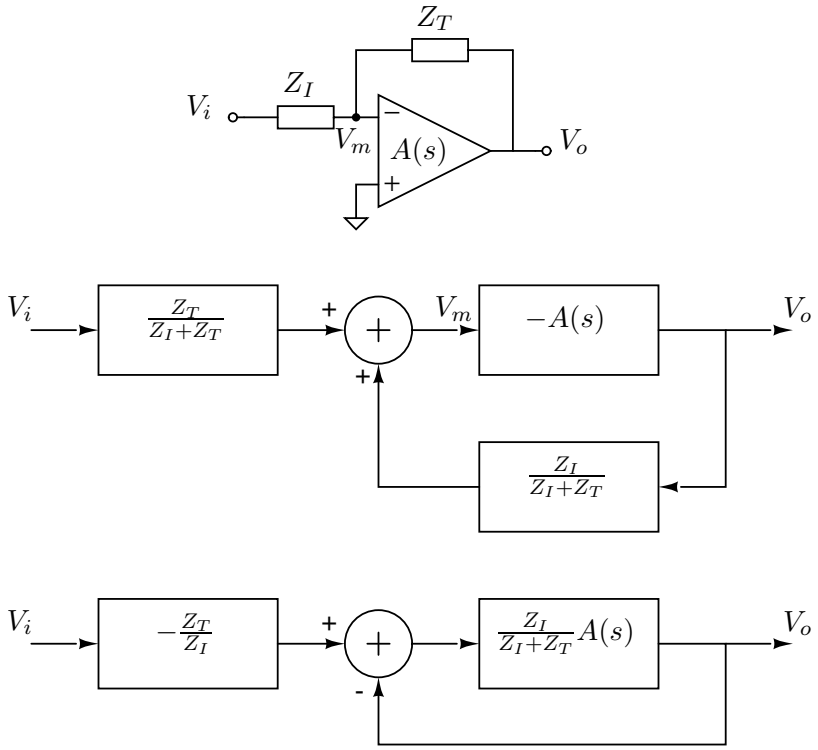

Figure B.4: Block diagram manipulations for determining L(s)

Equation B.3 defines the voltage of the inverting input as a superposition of the voltages contributed by the output and input voltages by means of their respective dividers.

Using this equation, we can draw a block diagram for the closed loop system. Manipulating this block diagram into a unity feedback configuration as shown in Figure B.4 allows us to easily discern the system loop transfer function L(s). The open loop gain A(s) can be determined by inspection from the device data sheet.

From the Bode plot of L(s) in Figure B.5 we can determine that at crossover, or when the magnitude of the loop transfer function equals 1, the phase margin is approximately negative 30 degrees. This is a good metric for indicating stability of a feedback system. For a stable system, we would like a phase margin of at least plus 45 degrees.

There are compensation tricks we can attempt which stabilize the system. Reducing the gain for example, could force a crossover close to resonance, where we have more phase. Techniques like this are very sensitive and difficult to implement successfully because they rely on such a fine adjustment of gain.

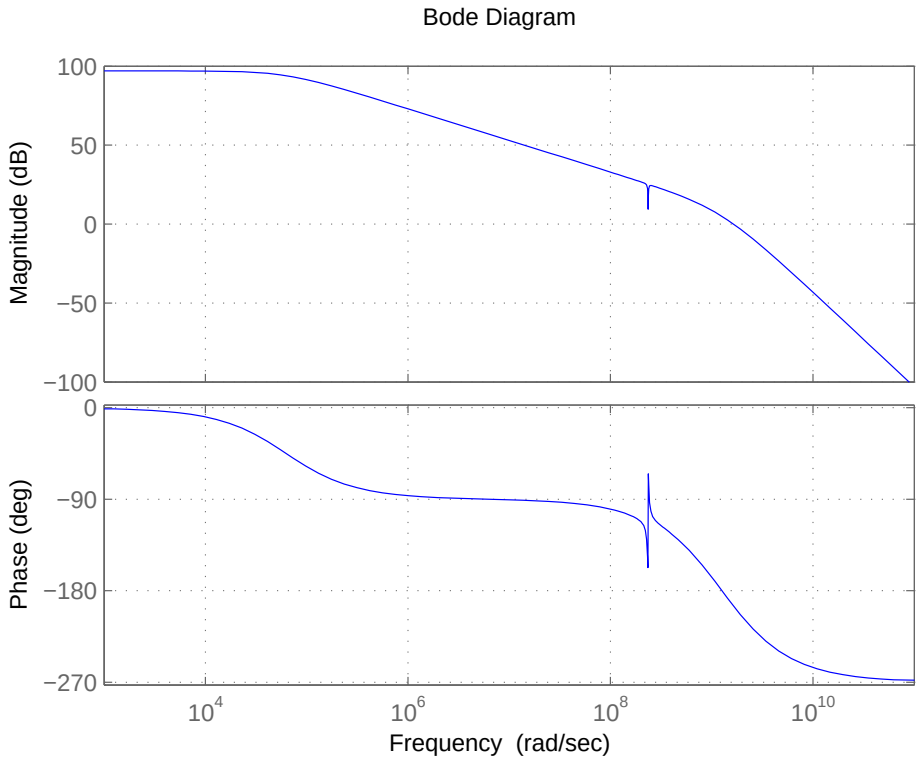

Figure B.5: Bode diagram of the loop transfer function

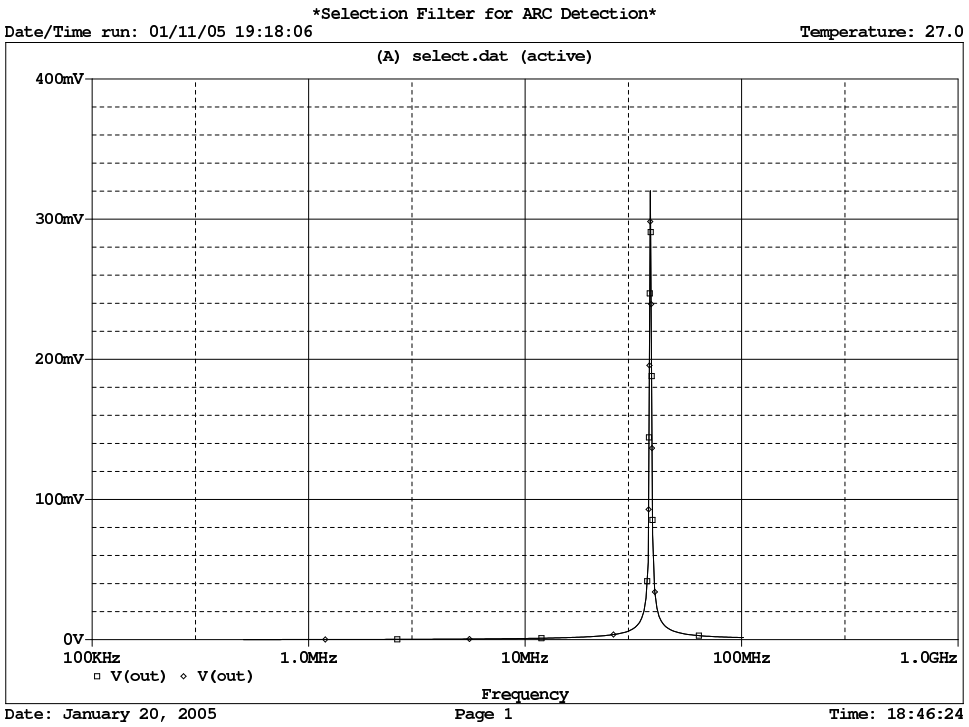

Figure B.6: SPICE probe output of AC Sweep of active filter in Figure B.2; $|V_{in}| = 100\text{mV}$

Appendix C

Partial Datasheet for the LTC5507

This appendix includes a partial datasheet for the Linear Technology 100 kHz to 1 GHz RF Power Detector, part LTC5507. This component was used in our detector design. The pages included here allow the reader to understand the basic operation of the device and its ratings and specifications. Not included here are pages describing a demonstration board schematic, packaging geometry, and a related parts listing.

LTC5507

100kHz to 1GHz RF Power Detector

FEATURES

- **Temperature Compensated Internal Schottky Diode RF Detector**
- **Wide Input Power Range: –34dBm to 14dBm**
- **Ultra Wide Input Frequency Range: 100kHz to 1000MHz**
- **Buffered Output**
- **Wide V_{CC} Range of 2.7V to 6V**
- Low Operating Current: 550µA
- Low Shutdown Current: <2µA
- Low Profile (1mm) ThinSOT™ Package

APPLICATIONS

- Wireless Transceivers
- Wireless and Cable Infrastructure
- RF Power Alarm
- Envelope Detector

DESCRIPTION

The LTC®5507 is an RF power detector for applications operating from 100kHz to 1000MHz. The input frequency range is determined by an external capacitor. A temperature-compensated Schottky diode peak detector and buffer amplifier are combined in a small 6-pin ThinSOT package.

The RF input voltage is peak detected using an on-chip Schottky diode and external capacitor. The detected voltage is buffered and supplied to the V_{OUT} pin. A power saving shutdown mode reduces supply current to less than 2µA.

TYPICAL APPLICATION

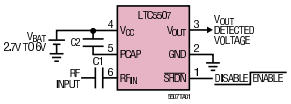

Figure 1. 100kHz to 1000MHz RF Power Detector

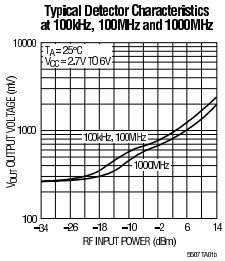

Figure C.1: LTC5507 Datasheet Page 1

ABSOLUTE MAXIMUM RATINGS

(Note 1)

V_{CC}, V_{OUT} to GND ..... –0.3V to 6.5V
RF_{IN} Voltage to GND ..... (V_{CC} ±1.8V) to 7V
$\overline{SHDN}$ Voltage to GND ..... –0.3V to (V_{CC} + 0.3V)
PCAP Voltage to GND ..... (V_{CC} – 1.8V) to 7V
I_{VOUT} 5mA
Operating Temperature Range (Note 2) .. –40°C to 85°C
Maximum Junction Temperature ..... 125°C
Storage Temperature Range ..... –65°C to 150°C
Lead Temperature (Soldering, 10 sec)..... 300°C

PACKAGE/ORDER INFORMATION

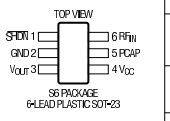

S6 PACKAGE
6-LEAD PLASTIC SOT-23

T_{JMAX} = 125°C, θ_{JA} = 250°C/W

ORDER PART NUMBER
LTC5507ES6
S6 PART MARKING
LTZX

Consult LTC Marketing for parts specified with wider operating temperature ranges.

ELECTRICAL CHARACTERISTICS

The ● denotes the specifications which apply over the full operating temperature range, otherwise specifications are at T_A = 25°C. V_{CC} = 3.6V, RF Input Signal is Off, unless otherwise noted.

PARAMETER	CONDITIONS		MIN	TYP	MAX	UNITS
V_{CC} Operating Voltage		●	2.7		6	V
I_{VCC} Shutdown Current	$\overline{SHDN}$ = 0V	●			2	µA
I_{VCC} Operating Current	$\overline{SHDN}$ = V_{CC}, I_{VOUT} = 0mA	●		0.55	0.85	mA
V_{OUT} V_{OL} (No RF Input)	R_{LOAD} = 2k, $\overline{SHDN}$ = V_{CC}, Enabled $\overline{SHDN}$ = 0V, Disabled		130	250 1	370	mV mV
V_{OUT} Output Current	V_{OUT} = 1.75V, V_{CC} = 2.7V to 6V, ΔV_{OUT} = 10mV	●	1	2		mA
V_{OUT} Enable Time	$\overline{SHDN}$ = V_{CC}, C_{LOAD} = 33pF, R_{LOAD} = 2k	●		7	20	µs
V_{OUT} Load Capacitance	(Note 4)	●			33	pF
V_{OUT} Noise	V_{CC} = 3V, Noise BW = 1.5MHz, 50Ω RF Input Termination			2		mV_{P-P}
$\overline{SHDN}$ Voltage, Chip Disabled	V_{CC} = 2.7V to 6V	●			0.35	V
$\overline{SHDN}$ Voltage, Chip Enabled	V_{CC} = 2.7V to 6V	●	1.4			V
$\overline{SHDN}$ Input Current	$\overline{SHDN}$ = 3.6V	●		24	40	µA
RF_{IN} Input Frequency Range				0.1– 1000		MHz
Max RF_{IN} Input Power	(Note 3)			14		dBm
RF_{IN} AC Input Resistance	F = 10MHz, RF Input = –10dBm F = 1000MHz, RF Input = –10dBm			130 95		Ω Ω
RF_{IN} Input Shunt Capacitance				1.7		pF

Note 1: Absolute Maximum Ratings are those values beyond which the life of a device may be impaired.

Note 2: Specifications over the –40°C to 85°C operating temperature range are assured by design, characterization and correlation with statistical process controls.

Note 3: RF performance is tested at: 80MHz, –4dBm

Note 4: Guaranteed by design.

Figure C.2: LTC5507 Datasheet Page 2

TYPICAL PERFORMANCE CHARACTERISTICS

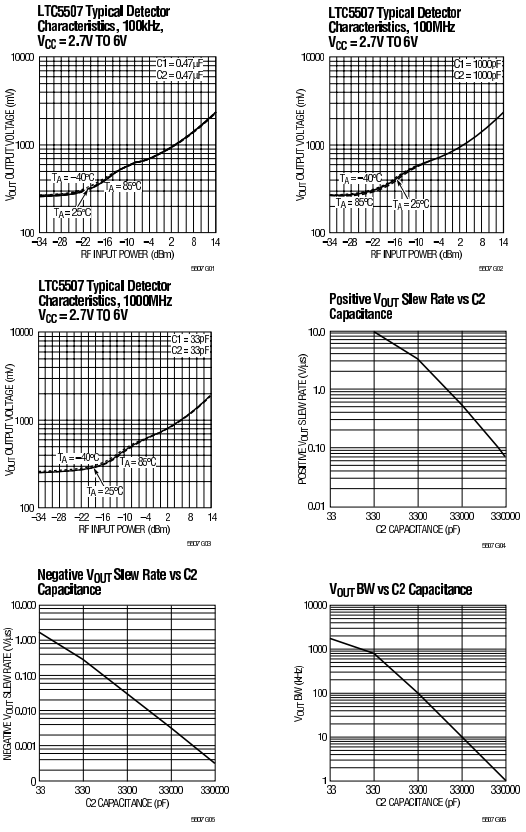

Figure C.3: LTC5507 Datasheet Page 3

PIN FUNCTIONS

$\overline{SHDN}$ (Pin 1): Shutdown Input. A logic low or no-connect on the $\overline{SHDN}$ pin places the part in shutdown mode. A logic high enables the part. $\overline{SHDN}$ has an internal 150k pull down resistor to ensure that the part is in shutdown when the enable driver is in a tri-state condition.

GND (Pin 2): System Ground.

V_{OUT} (Pin 3): Buffered and Level Shifted Detector Output Voltage.

V_{CC} (Pin 4): Power Supply Voltage, 2.7V to 6V. V_{CC} should be bypassed with 0.1µF and 100pF ceramic capacitors.

PCAP (Pin 5): Peak Detector Hold Capacitor. Capacitor value is dependent on RF frequency. Capacitor must be connected between PCAP and V_{CC}.

RF_{IN} (Pin 6): RF Input Voltage. Referenced to V_{CC}. A coupling capacitor must be used to connect to the RF signal source. This pin has an internal 250Ω termination and an internal Schottky diode detector.

BLOCK DIAGRAM

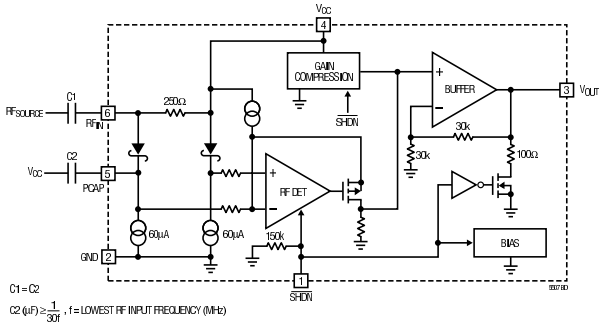

Figure 2.

Figure C.4: LTC5507 Datasheet Page 4

APPLICATIONS INFORMATION

Operation

The LTC5507 integrates several functions to provide RF power detection over frequencies up to 1000MHz. These functions include an internally compensated buffer amplifier, an RF Schottky diode peak detector and level shift amplifier to convert the RF signal to DC, a delay circuit to avoid voltage transients at V_{OUT} when coming out of shutdown, and a gain compression circuit to extend the detector dynamic range.

Buffer Amplifier

The buffer amplifier has a gain of two and is capable of driving a 2mA load. The buffer amplifier typically has an output voltage range of 0.25V to V_{CC} – 0.1V.

RF Detector

The internal RF Schottky diode peak detector and level shift amplifier converts the RF input signal to a low frequency signal. The frequency range of the RF pin is typically up to 1000MHz. The detector demonstrates excellent operation over a wide range of input power. The Schottky detector is biased at about 70µA. The hold capacitor is external.

Gain Compression

The gain compression circuit changes the feedback ratio as the RF peak-detected input voltage increases above 60mV. Below 60mV, the DC voltage gain from the peak detector to the buffer output is 4. Above 140mV, the DC voltage gain is reduced to 0.75. The compression expands the low power detector range due to higher gain.

Modes of Operation

MODE	$\overline{SHDN}$	OPERATION
Shutdown	Low	Disabled
Enable	High	Power Detect

Applications

The LTC5507 can be used as a self-standing signal strength measuring receiver for a wide range of input signals from –34dBm to 14dBm for frequencies up to 1000MHz.

The LTC5507 can be used as a demodulator for AM and ASK modulated signals with data rates up to 1.5MHz. Depending on specific application needs, the RSSI output can be split into two branches, providing AC-coupled data (or audio) output and DC-coupled, RSSI output for signal strength measurements and AGC.

C1, C2 Capacitor Selection (Refer to Figure 3)

C1 couples the RF input signal to the detector input RF_{IN} which is referenced to V_{CC}. C2 is the peak detector capacitor connected between PCAP and V_{CC}. The value of C2 will affect the slew rate and bandwidth. Typically C1 can equal C2. Ceramic capacitors are recommended for C1 and C2. The values for C1 and C2 are dependent on the operating RF frequency. The capacitive reactance should be less than 5Ω to minimize ripple on C2.

$C2(\mu F) \geq 1/(30 \bullet f)$ where f is the lowest RF input frequency (MHz)

$C1 = C2$

In general, select C1 and C2 large enough to pass the lowest expected RF signal frequency, as described by the above formulas. But optimize C1 and C2, subject to this constraint, to improve output slew rate and bandwidth, and to enable good AC performance for the highest expected RF signal frequency.

Figure C.5: LTC5507 Datasheet Page 5

Appendix D

Decibel Scaling on the Spectrum Analyzer and related equipment

---

The 50 Ω impedance at the input of the spectrum analyzer is the basis of all measurements taken with the instrument. When we perform a frequency sweep, we can elect to view frequency information either as a voltage across the input impedance, or as a power dissipated in the input impedance. On the Agilent 4395A we can choose display units of linear (Watts, Volts) or logarithmic (dBm, dBV, dBμV) form.

While the linear measurements are straightforward, logarithmic measurments are often mixed together or confused with one another. The decibel is a relative unit, not an absolute measurement. This means measurements are made as a ratio to an absolute reference. The references are specified as follows:

dBm: decibels referenced to 1 milliwatt (RMS)
dBV: decibels referenced to 1 volt (RMS)
dBμV: decibels referenced to 1 microvolt (RMS)
dBc: decibels referenced to a carrier signal (not on analyzer)

The following equations are used to define and to convert among these units.

$$Voltage[dB\mu V] = 20\log\left(\frac{RMS\,Voltage\,[volts]}{1\mu V}\right) \tag{D.1}$$

$$Voltage[dBV] = 20\log\left(\frac{RMS\,Voltage\,[volts]}{1V}\right) \tag{D.2}$$

$$Power[dBm] = 10\log\left(\frac{RMS\,Power\,[Watts]}{1mW}\right) \tag{D.3}$$

To get a sense of these units, it is useful to imagine a basic example. One watt is 1000 times 1 milliwatt. 10 log 1000 is 30. In other words, 1 Watt is 30 decibels above 1 milliwatt (or 0 dBm).

By this logic, if we are viewing in units of dBV, a factor of 10 change of the input voltage will correspond to a change of 20 dBV. If the scaling on the analyzer is set to 10 dB per division, this factor of 10 will then correspond to a change of 2 divisions. If however, the scaling is set to 20 dB per division, then we will see a change of 1 division.

If we are viewing in units of dBm, a factor of 10 change in input power will correspond to a factor of 10 change in dBm. For the same scaling of 10 dB per division, this corresponds to a change of 1 division.

Other useful equations to note when performing tests on the spectrum analyzer include

$$Power_{in} = \frac{{Voltage_{in}}^2}{R_{in}} \tag{D.4}$$

$$RMS\,Voltage = \frac{Peak\,Voltage}{\sqrt{2}} = \frac{Peak\,to\,Peak\,Voltage}{2\sqrt{2}} \tag{D.5}$$

As an example of this definition and analysis, we apply two signals which differ by an amplitude factor of $\sqrt{10}$ (0.105 and 0.331 Volts peak to peak) to the 50 ohm input of the spectrum analyzer. Converting to RMS power using Equations D.4 and D.5, we calculate respective dissipation powers of $2.7{\cdot}10^{-5}$ Watts and $2.7{\cdot}10^{-4}$ Watts respectively. This factor of 10 change in power is visible as the movement of the frequency peaks in figures D.1 and D.2 by one vertical division. The values of spectral power at the peaks are related to the input voltages by equation D.3.

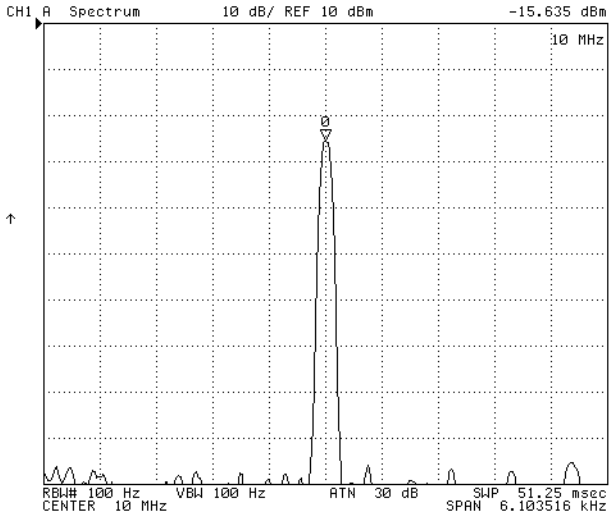

Figure D.1: Spectral Sweep: .105 Vpp input, -15.6 dBm peak

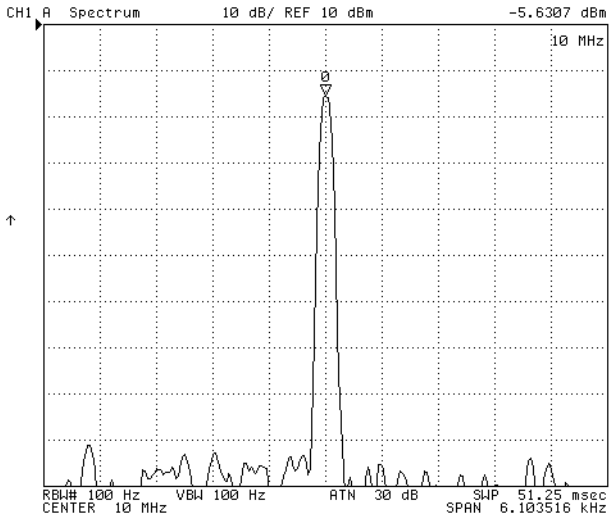

Figure D.2: Spectral Sweep: .331 Vpp input, -5.6 dBm peak

Appendix E

SAE Table 5 and Calculations

These calculations estimate the number of noise sources necessary to begin to interfere with the detection of an arc. A detailed explanation of this calculation is found in Section 4.3.2 for SAE J1113/41 Class 1 Loads.

Class	0.15-0.3 MHz	0.53-2.0 MHz	5.9-6.2 MHz	30-54 MHz	70-108 MHz
1	90	66	57	52	42
2	80	58	51	46	36
3	70	50	45	40	30
4	60	42	39	34	24
5	50	34	33	28	18

Table E.1: Table 5 from [12]; Narrowband noise limits for automotive loads

Corresponding voltages V across 50 Ω:

$$V[volts] = \frac{1}{10^6} \cdot 10^{\frac{V[dB\mu V]}{20}} \tag{E.1}$$

Class	0.15-0.3 MHz	0.53-2.0 MHz	5.9-6.2 MHz	30-54 MHz	70-108 MHz
1	0.031623	0.001995	0.000708	0.000398	0.000126
2	0.010000	0.000794	0.000355	0.000200	0.000063
3	0.003162	0.000316	0.000178	0.000100	0.000032
4	0.001000	0.000126	0.000089	0.000050	0.000016
5	0.000316	0.000050	0.000045	0.000025	0.000008

Table E.2: Corresponding Voltage [V] level across 50 Ω

For the 30-54 MHz range, the number of loads N producing uncorrelated noise in a single 120 kHz band required to produce enough noise to mask half of the arcing signal (signal to noise ratio of 2 to 1):

$$N = \left(\frac{Arc\ Noise\ Level}{Load\ Noise\ Level} \right)^2 \tag{E.2}$$

Class	0.15-0.3 MHz	0.53-2.0 MHz	5.9-6.2 MHz	30-54 MHz	70-108 MHz
1				21.77	
2				86.68	
3				345.10	
4				1373.85	
5				5469.40	

Table E.3: Number of noisy loads N necessary to mask arcing emissions

Appendix F

Schematics and PCB Layout

This section contains schematics and PCB layout designs for both the original and final detector designs. All PCB layouts were created using Eagle CAD layout software.

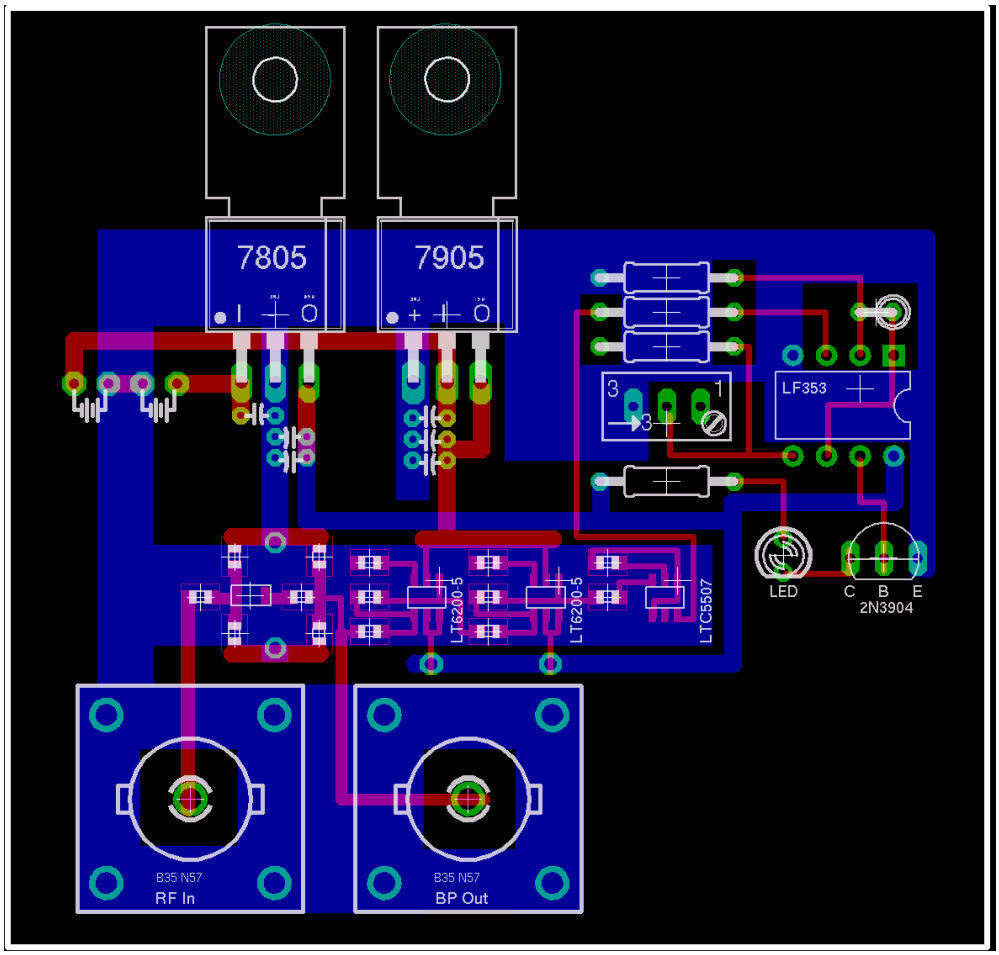

Figure F.1: Voltage based detector PCB layout

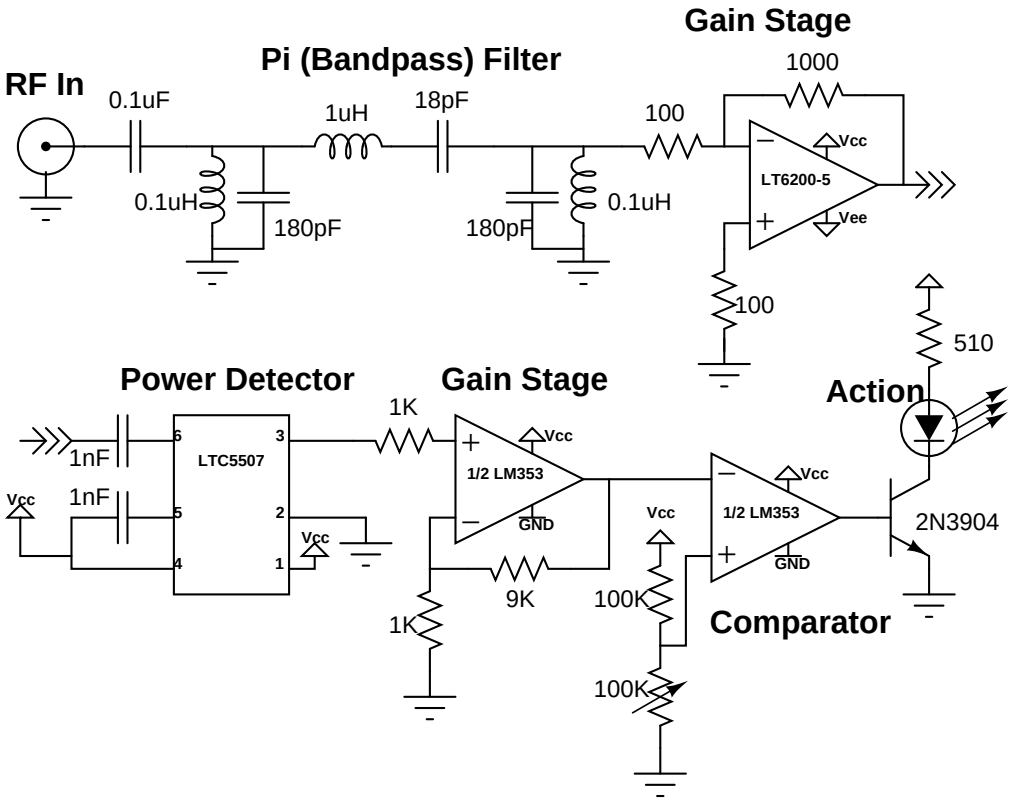

Figure F.2: Schematic for original voltage based detector

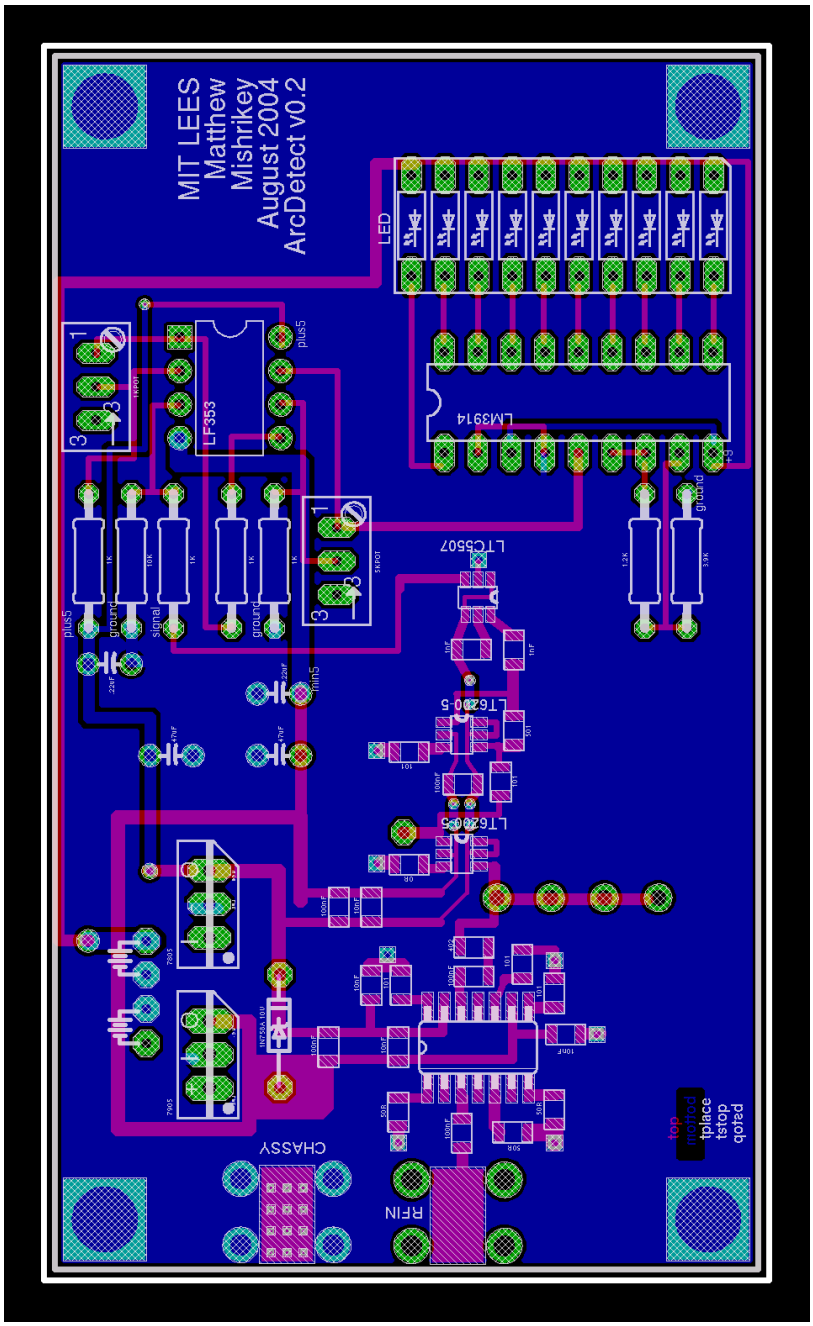

Figure F.3: Final detector PCB layout with ground plane

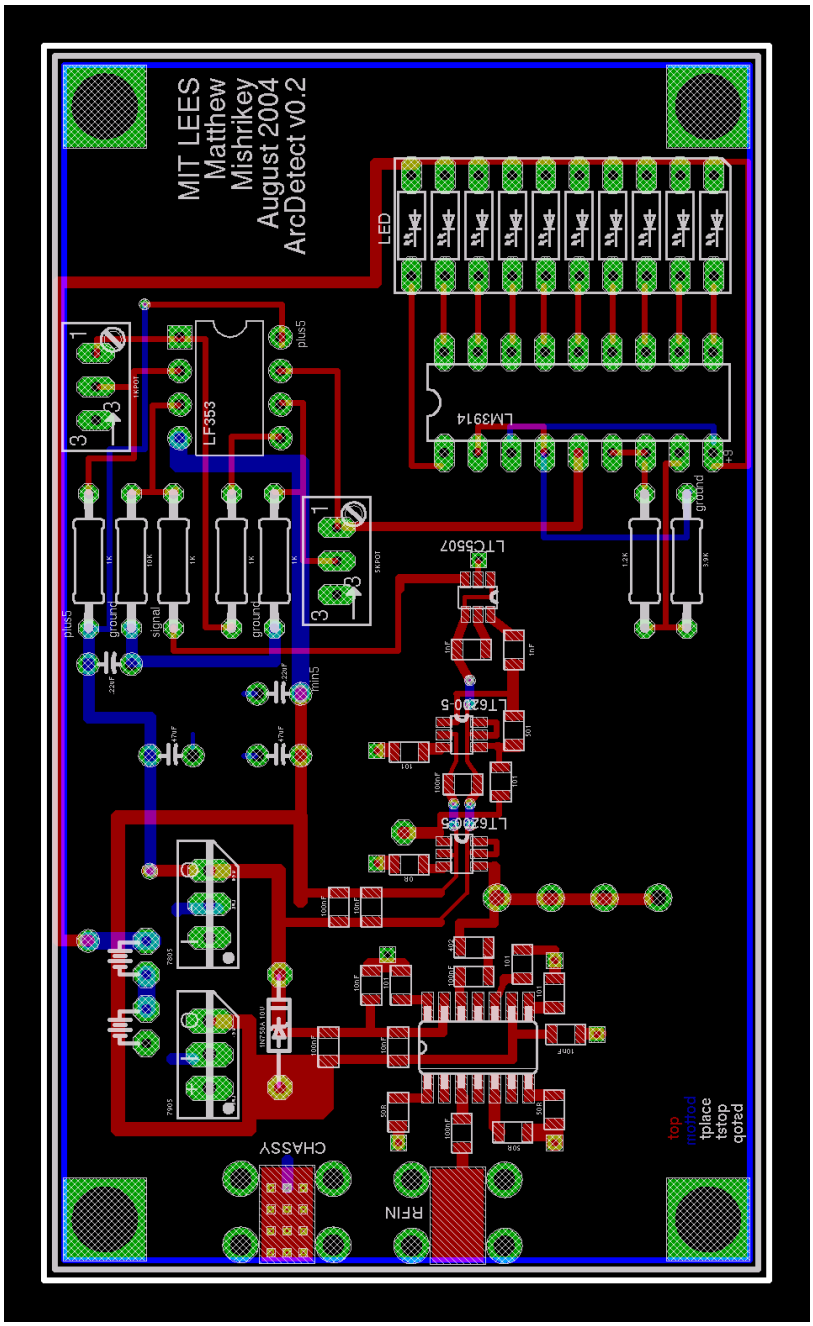

Figure F.4: Final detector PCB layout without ground plane

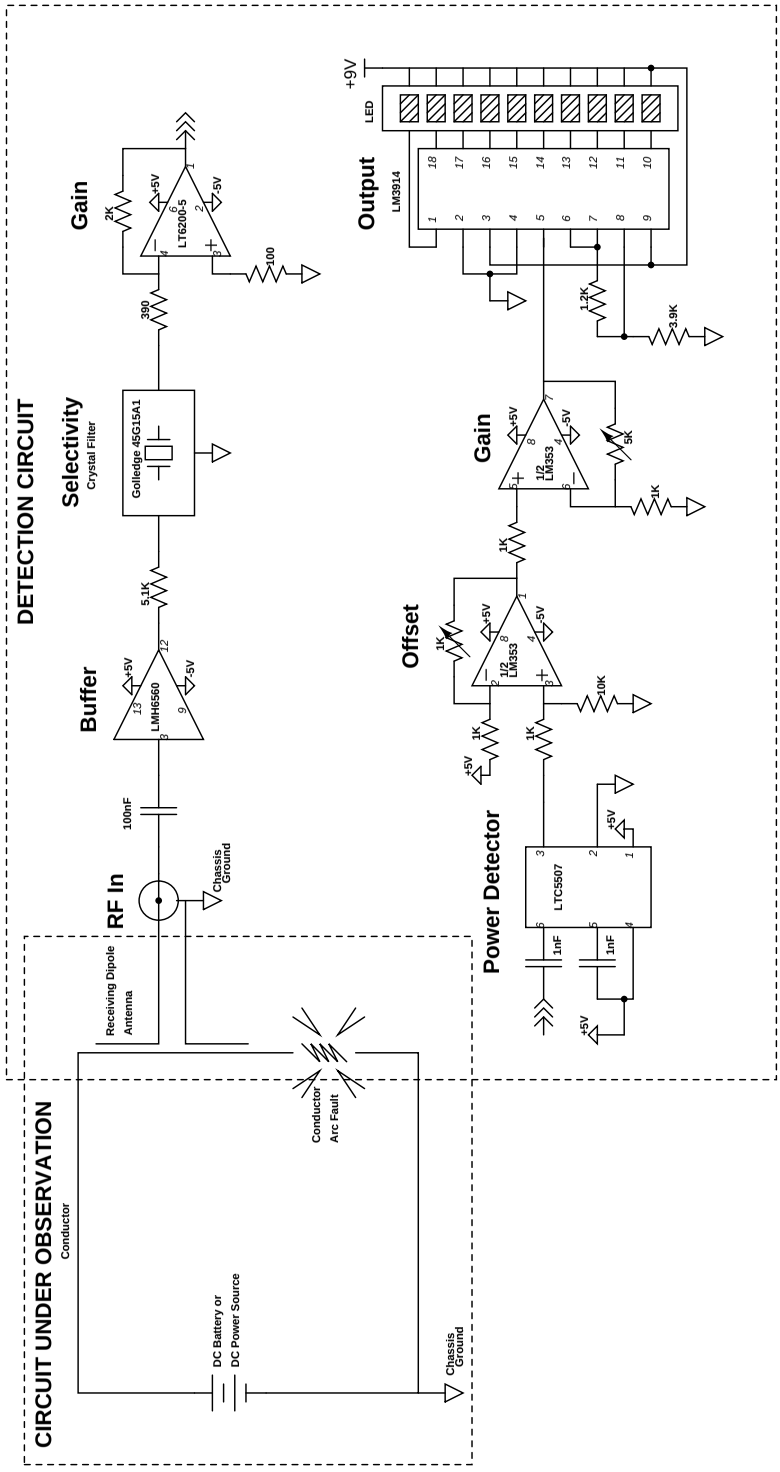

Figure F.5: Schematic for final detector design, repeated from 5.1

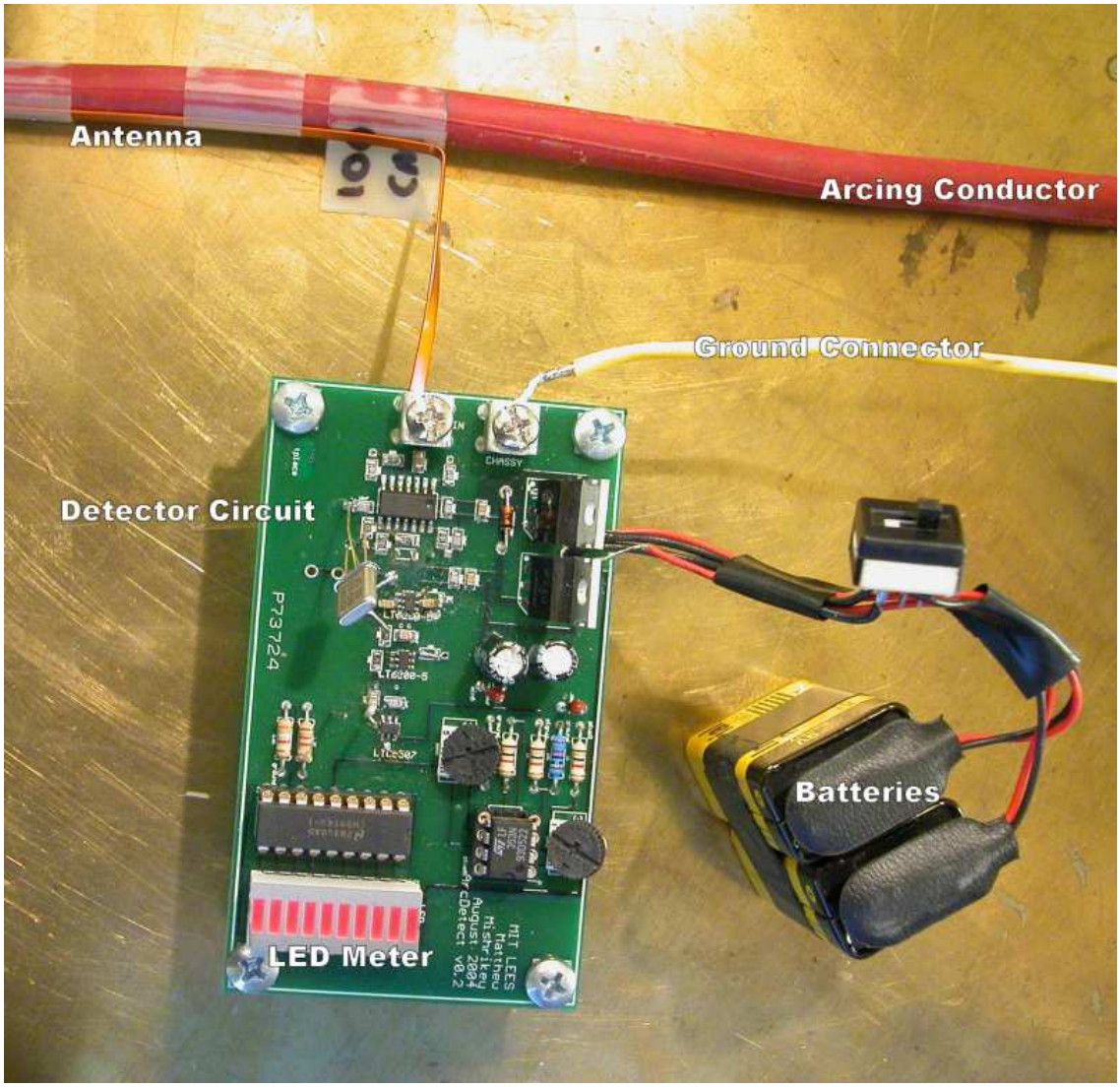

Figure F.6: Detector photograph, repeated from Figure 7.3

Bibliography

[1] Sam Y. Guo, James L. Jones III, and Ansel S. Dooley. US Patent 6,683,766: DC arc detection and prevention circuit and method, January 2004.

[2] Ragnar Holm. *Electric Contacts, Theory and Application*. Springer-Verlag New York Inc., New York, fourth edition, 1967.

[3] Honeywell Inc. Hall Effect Sensing and Application Book *http* : *//content.honeywell.com/sensing/prodinfo/solidstate/technical/chapter*2.*pdf*. Online, 2004.

[4] Howard M. Ham Jr. and James J. Keenan. US Patent 5,477,150: Electric arc and radio frequency spectrum detection, 1995.

[5] David J. Klassen and Edward G. Anderson. US Patent 5,268,644: Fault detection and isolation in automotive wiring harness by time-domain reflectometry, April 1990.

[6] Thomas H. Lee and Ali Hajimiri. Oscillator phase noise: a tutorial. In *IEEE Journal of Solid-State Circuits*, volume 35, pages 326–336, March 2000.

[7] Golledge Electronics Ltd. Golledge GMCF45 crystal filter specifications *http* : *//www.golledge.co.uk/docs/products/fil_xtl/gmcf*45.*htm*. Online, 2004.

[8] Joseph Luis. Detection of electric arcs in 42 volt automotive systems. Master's project, Massachusetts Institute of Technology, EECS Department, May 2003.

[9] James A. Momoh and Robert M. Button. Design and analysis of aerospace DC arcing faults using fast fourier transformation and artificial neural network. In *IEEE Power Engineering Society General Meeting*, volume 2, page 793, July 2003.

[10] National Fire Protection Agency (NFPA). NFPA 70 national electric code. NFPA Publication, 2002.

[11] Ole Nykjaer. 21-30 Mhz Preamplifier for HF *http* : *//hjem.get*2*net.dk/ole_nykjaer/oz*2*oe/hfpreamp/hfpreamp.html*. Online, 2000.

[12] Society of Automotive Engineers Inc. Standard SAE J1113/41: Limits and methods of measurement of radio disturbance characteristics of components and modules for the protection of receivers used on-board vehicles, September 1994.

[13] Michael Perrott. Lecture 12: Noise in voltage controlled oscillators *http* : *//stellar.mit.edu/s/course*/6/*sp*04/6.976/*materials.html*. Online, 2004.

[14] Dana G. Reed, editor. *The ARRL Handbook for Radio Communications*. American Radio Relay League, Connecticut, eighty-first edition, 2004.

[15] J. H. Rogers, P. LaRue, D. A. Phelps, and R. I. Pinsker. RF arc detection using harmonic signals. In *Proc. 16th IEEE/NPSS Symposium*, volume 1 of *Fusion Engineering*, 1995.

[16] Thomas J. Schoepf, Malakondaiah Naidu, and Suresh Gopalakrishnan. Mitigation and analysis of arc faults in automotive DC networks. In *Proceedings of the Forty-Ninth IEEE Holm Conference on Electrical Contacts*, pages 163–171, September 2003.

[17] Gary W. Scott. US Patent 6,782,329: Detection of arcing faults using bifurcated wiring system, August 2004.

[18] David Talbot. A new 42 volt standard. *Technology Review*, 2002.

[19] Mac E. Van Valkenburg and Rolf Schaumann. *Design of Analog Filters*. Oxford University Press, second edition, 2001.

[20] M. Vaughan and P.J. Moore. A nonintrusive power system arcing fault location system utilising the VLF radiated electromagnetic energy. In *Power Engineering Society Winter Meeting*, volume 4 of *Fusion Engineering*, pages 2334–2448, January 2000.

[21] M. Vaughan, P.J. Moore, and E.J. Bartlett. Investigations into electromagnetic emissions from power system arcs. In *International Conference and Exhibition on Electromagnetic Compatibility*, pages 47–52, July 1999.

[22] Alan Nuo-Bei Wu. Investigation of electric arcs in 42-volt automotive systems. Master's project, Massachusetts Institute of Technology, EECS Department, June 2001.